Targeting autophagy potentiates tyrosine kinase inhibitor-induced cell death in Philadelphia positive cells including primary CML stem cells

Cristian Bellodi[1,8], Maria Rosa Lidonnici[2,8], Ashley Hamilton[3,8], G. Vignir Helgason[3],Angela Rachele Soliera[2], Mattia Ronchetti[2], Sara Galavotti[1], Kenneth W. Young[1], Tommaso Selmi[1], Richard A. Van Etten[4], Nick Donato[5], Ann Hunter[6], David Dinsdale[1], Elena Tirro'[7], Paolo Vigneri[7], Pierluigi Nicotera[1], Martin J. Dyer[1], Tessa Holyoake[3], Paolo Salomoni[1]* and Bruno Calabretta[2]*

[1]MRC Toxicology Unit, Leicester, United Kingdom; [2]Kimmel Cancer Center, Thomas Jefferson University, Philadelphia, USA; [3]Paul O'Gorman Leukaemia Research Centre, University of Glasgow, Gartnavel General Hospital, Glasgow, United Kingdom; [4]Molecular Oncology Research Institute and Division of Hematology/Oncology, Tufts-New England Medical Center, Boston, USA; [5]Division of Hematology/Oncology, University of Michigan, Comprehensive Cancer Center, USA; [6]Department of Pathology, Royal Infirmary Hospital, Leicester, United Kingdom; [7]Department of Biomedical Sciences, University of Catania, Catania, Italy.

*To whom the correspondence should be addressed. E-mail:

Bruno.Calabretta@mail.jci.tju.edu

ps90@le.ac.uk

[8]These authors contributed equally to this work

Abstract

Imatinib mesylate (IM), a potent ATP-competitive inhibitor of the BCR/ABL tyrosine kinase, has become standard first-line therapy for patients with chronic myeloid leukemia (CML), but the frequency of resistance increases in advancing stages of disease. Elimination of BCR/ABL-dependent intracellular signals triggers apoptosis, but it is unclear whether this activates additional cell survival and/or death pathways. We show that IM induces autophagy in CML blast crisis cell lines, CML primary cells and $p210^{BCR/ABL}$-expressing 32Dcl3 (32D) myeloid precursor cells, but not in 32D cells expressing v-Src or the IM-resistant T315I $p210^{BCR/ABL}$ mutant. IM-induced autophagy does not involve c-Abl, as it is also observed in cells co-expressing $p210^{BCR/ABL}$ and the IM-resistant T315I c-Abl mutant. Induction of autophagy is associated with endoplasmic reticulum-stress and is suppressed by depletion of intracellular calcium. By contrast, ectopic Bcl-2 expression does not block IM-induced autophagy. Suppression of autophagy by pharmacological inhibitors or RNA interference of essential autophagy genes enhances cell death induced by IM in cell lines and primary CML cells, demonstrating that induction of autophagy has a pro-survival effect. Critically, the combination of tyrosine kinase inhibitors (TKI) with inhibitors of autophagy results in near complete elimination of phenotypically (CD34+CD38-) and functionally (colony forming and long-term culture-initiating cells) defined CML stem cells**.** Together, these findings suggest that autophagy inhibitors may enhance the therapeutic effects of TKI in the treatment of CML.

Introduction

Chronic myeloid leukemia (CML) is a malignancy arising from transformation of the hematopoietic stem cell which typically evolves through three distinct disease stages: an indolent chronic phase (CP) characterized by the accumulation of mature granulocytes and myeloid precursors in the bone marrow and the peripheral blood; an accelerated phase (AP) characterized by an increase in disease burden and in the frequency of progenitor/precursor cells and an acute phase called blast crisis (BC) marked by increasing numbers of differentiation-arrested blast cells (1-3). The hallmark of all phases is the Philadelphia (Ph^1) chromosome, a reciprocal translocation of chromosomes 9 and 22, which generates the *BCR/ABL* fusion gene encoding a constitutively active tyrosine kinase (4). $p210^{BCR/ABL}$ exerts its oncogenic function by activating a cascade of intracellular signalling pathways which leads to increased survival and proliferation and limited dependence on growth factors (5, 6). Two of the major pathways activated by BCR/ABL are the class I phosphatidylinositol-3 kinase (PI-3K) and the Ras pathways (7, 8), which are deregulated in most human cancers (9, 10). In normal hematopoietic cells, these two pathways are activated by stimulation of growth factor receptors with intrinsic or JAK-associated tyrosine kinase activity, suggesting that $p210^{BCR/ABL}$ effectively mimics growth factor-dependent signalling.

The generation of the BCR/ABL kinase ATP-competitive inhibitor imatinib mesylate (IM) has revolutionized the therapy of CML, since this drug is highly effective in the CP of the disease (11). However, there are three major problems with IM-based therapy: i) the limited response of CML-BC or Ph^1 B-acute lymphoblastic leukemia (ALL) patients to IM (11-13); ii) the development of resistance caused in approximately 40% of cases by mutations in the BCR/ABL kinase domain which impair the ability of IM to interact with the protein (14-18); and iii) the relative insensitivity of Ph^1 CML stem cells to IM (19). For these reasons, more potent BCR/ABL inhibitors, also targeting IM-resistant mutants, are being developed and tested (20, 21). However, at least one common BCR/ABL mutant (carrying the T315I mutation) is resistant to all tyrosine kinase inhibitors (TKI) developed so far (22). A further limitation is that primitive Ph^1 stem cells overexpress wild type $p210^{BCR/ABL}$ and appear to be intrinsically resistant not only to treatment with IM but also to second generation (dasatinib, nilotinib and bosutinib) TKI (19,23-27). Therefore,

there is the need to develop new therapeutic approaches that, in combination with TKI, might be more effective in preventing the outgrowth of TKI-resistant CML/Ph[1] ALL cells and target the stem cell population.

Macroautophagy (hereafter referred to as autophagy) is a degradative process in eukaryotic cells that results in the breakdown of intracellular material within lysosomes under homeostatic conditions or in response to stress signals (28, 29), allowing cells to adapt to environmental and/or developmental signals. Autophagy is a genetically controlled process which progresses through definite steps leading to the engulfment of long-lived proteins and whole organelles into multi-membraned vacuoles called autophagosomes (28, 29). Autophagosomes then fuse with lysosomes for final destruction and recycling (28, 29). While in certain cellular contexts autophagy can serve as an alternative cell death mechanism, named type II cell death (30-32), it is becoming increasingly clear that this process can also act as a cell survival mechanism. In fact, autophagy is a process by which cells can adapt their metabolism to starvation caused by a decrease in metabolite concentrations or extracellular nutrients, a typical consequence of loss of growth factor signalling (32, 33), allowing cells to evade programmed cell death (32, 33). Accordingly, inhibition of autophagy by knockdown of autophagy genes or by use of pharmacological inhibitors such as chloroquine (CQ, an inhibitor of lysosomal acidification (34)), results in cell death of growth factor-starved cells in which apoptosis has been genetically ablated (33, 35). In tumors displaying defective apoptosis, inhibition of autophagy causes caspase-independent necrotic cell death, which, in turn, augments inflammation, leading to enhanced tumor burden (36). In two recent studies, treatment of Myc-induced lymphomas with the autophagy inhibitor CQ, resulted in reduced tumor growth *in vivo* (34, 37), suggesting that induction of autophagy provides a protective mechanism in tumor cells. Thus, the consequences of autophagy inhibition are double-faced, as it can either promote or suppress tumorigenesis depending on the tumor type or inflammation status.

Another interesting aspect of autophagy is its involvement in the response to chemotherapy. Autophagy inhibition has been shown to sensitize tumor cells to cell death induced by irradiation (38-40), alkylating agents (41) or arsenic trioxide (42), suggesting that cancer cells can react to chemotherapy by inducing autophagy as a self-defence mechanism. How an increase in intracellular lysosome-mediated catabolism results in reduced sensitivity to cell death is still unclear. Perhaps,

clearance of mitochondria through autophagy (mitophagy) might cause a depletion of pro-apoptotic signals such as the release of cytochrome c (43, 44).

As mentioned above, $p210^{BCR/ABL}$ has the ability to activate several survival pathways, effectively mimicking growth factor signaling (5-8). This, in turn, causes transformed cells to acquire resistance to apoptosis induced by growth-factor deprivation (5-8). Inhibition of BCR/ABL tyrosine kinase activity by IM results in induction of cell death, which is caused by a sudden decrease of intracellular survival signals and a relative increase in pro-apoptotic signals (45, 46). We show here that apoptosis is not the sole consequence of BCR/ABL inhibition, as IM treatment rapidly activates an autophagic process, which follows the induction of endoplasmic reticulum (ER) stress and relies on intracellular calcium. Of greater importance, inhibition of autophagy by pharmacological inhibitors potentiates IM-induced cell death in CML cell lines and primary CML cells, including those carrying partially IM-resistant BCR/ABL mutants. Colony formation of candidate CML stem cells, defined as CD34+CD38- and LTC-IC, was also markedly suppressed by combination treatment. Knockdown of the autophagy genes Atg5 and Atg7 had comparable effects, supporting the specificity of the pharmacological inhibitors. These findings indicate that induction of autophagy provides a survival mechanism to IM-treated BCR/ABL-expressing cells, including the stem cell population, and strongly suggest that inhibition of autophagy may improve the therapeutic efficacy of TKI in the treatment of CML.

Results

IM induces autophagy in p210$^{BCR/ABL}$-expressing CML cell lines

IM induces death of CML cells, but additional effects have not been studied in detail. Therefore, we designed experiments to study cellular changes induced by IM in CML cells. To this end, the effects of IM treatment were initially analyzed in the erythro-megakaryocytic CML-BC line K562. To exclude effects due to apoptosis-related changes, cells were treated with zVADfmk, a pan-caspase inhibitor. Morphological analysis of K562 cells cultured for 24 hours in the presence of 2μM IM showed a consistent decrease in cell size as compared to cells treated with zVAD alone (Figure 1A). A closer examination showed that the cytoplasm of IM/zVAD-treated cells was severely reduced and almost entirely filled with several translucent vacuoles (Figure 1A). Flow cytometry of physical parameters of IM/zVAD-treated cells revealed the appearance of a distinct population of smaller and denser cells, compared to those treated with zVAD only (FSC-H and SSC-H parameters, Figure 1B yellow arrow). This population was clearly distinct from apoptotic cells, which are smaller and less dense, as shown in cultures treated with IM only (Figure 1B). Mean FSC-H was also decreased in IM/zVAD-treated cells (Figure 1C). Similar changes were observed at earlier time points in cells treated with IM alone (not shown). These morphological changes were reminiscent of those induced by growth factor deprivation in hematopoietic cells (33). A previous study showed that growth factor withdrawal activated autophagy in cells lacking the intrinsic apoptotic pathway and that this process was critical for maintaining cell survival (35). Thus, we investigated whether inhibition of BCR/ABL-dependent survival signals by IM treatment could also trigger autophagy. Autophagy is invariably associated with conversion of the microtubule-associated protein 1 light chain 3 (LC3), also known as Atg8, from the cytosolic-LC3-I to the autophagosome-associated LC3-II form (47). Increased levels of LC3-II were clearly detected in extracts of IM-treated K562 cells (Figure 1D, upper panel). Immunofluorescence (IF)/confocal microscopy showed an increase in LC3-positive vacuoles in IM-treated K562 cells (not shown). In cells transduced with a retrovirus encoding LC3 fused to the enhanced green fluorescence protein (eGFP-LC3), Western blot showed a clear accumulation of eGFP-LC3-II in protein extracts as early as 6 hours after treatment with 2μM IM (Figure 1D, lower panel). Nevertheless, LC3-II accumulation could be due to inhibition, rather than induction of autophagy. To

exclude this possibility, we analyzed endogenous LC3-II levels in IM-treated K562 cells in the presence of cloroquine (CQ), an autophagy blocker. If IM blocked autophagy, one would expect equal levels of LC3-II in CQ and CQ/IM treated cells. Instead, LC3-II expression was higher in CQ/IM-treated cells (Supplementary Figure 1), supporting an autophagy-inducing function of IM.

IF/confocal microscopy confirmed the presence of large eGFP-positive cytoplasmic vacuoles in cells treated with 2μM IM for 24 hours (Figure 1E, right panels). Conversely, untreated cells contained smaller eGFP-positive granules (Figure 1E, left panels), which are probably due to non-specific aggregation of over-expressed LC3 (48).

Electron microscopy (EM) was then performed to evaluate formation of autophagic structures. Examination of untreated K562 cells demonstrated the presence of multivesicular bodies (MVB) in the cytoplasm of approximately 40% of the cell profiles (Supplementary Figure 2A, B). These organelles ranged from 1-4μm in diameter and were characterised by the presence of numerous small vesicles, 25-100nm in diameter, together with a few slightly larger, more electron-dense inclusions containing a lipofuscin-like material. Treatment of K562 cells with 2μM IM for 6 hours resulted in a large increase in the size and prevalence of cytoplasmic vacuoles, most of which contained many electron-dense inclusions (Supplementary Figure 3A, B). Similar inclusions were present in small vacuoles distributed throughout the cytoplasm of the cells (Supplementary Figure 3A and Supplementary Figure 4A, B). Many of these lysosome-like organelles appeared to be fusing, both together and with the larger vacuoles (Supplementary Figure 4A, B). Untreated cells transduced with eGFP-LC3 and processed for immunogold cytochemistry exhibited a sparse and apparently non-specific distribution of gold particles throughout the cytoplasm (data not shown). Conversely, cells treated with 2μM IM for 6 hours showed a definite concentration of GFP-labelling over the dense inclusions present in the cytoplasm and in the large vacuoles (Supplementary Figure 3C, D). Surprisingly, although the label was concentrated over the contents of these inclusions, their membrane was almost devoid of label. These results are consistent with the observations of Fader *et al.* (49), who reported the presence of constitutive MVBs in K562 cells. They also observed that the induction of autophagy led to increased interaction of MVBs with autophagosomes to yield hybrid organelles containing vesicles, which are labelled for

LC3. The presence of dense, lipofuscin-like material in the small cytoplasmic vacuoles, within 6 hours of treatment, probably indicates their rapid fusion with lysosomes and subsequent breakdown.

Cell shrinkage and induction of autophagy was confirmed also in the CML-lymphoid BC cell line BV173, which was chosen because of the slow kinetics of cell death induction upon IM treatment. May-Grünwald staining and FACS analysis of BV173 cells cultured for 72 hours in the presence 4μM IM revealed a decrease in cell size, compared to that of untreated cells (Supplementary Figure 5A, B). The cytoplasm of treated cells was severely reduced and filled with translucent vacuoles (Supplementary Figure 5A). Because of the slow kinetics of cell death it was not necessary to treat BV173 with zVADfmk, confirming that the reduction in cell size was not caused by caspase inhibition. Accumulation of LC3-II was clear only upon treatment with CQ, which blocks degradation of autophagosomes inside autolysosomes (Supplementary Figure 5C) (33, 34). Levels of LC3-II were higher in CQ/IM-treated cells than in CQ-treated cells, thus confirming the autophagy-inducing effect of IM. The same treatment demonstrated an accumulation of LC3-positive structures by IF/confocal microscopy (Supplementary Figure 5D) and EM (Supplementary Figure 6). This possibly reflects a very high rate of lysosome-mediated autophagosome degradation resulting in very high turnover of LC3-II in these cells.

In control experiments a reduction in cell size was observed in IL-3-starved myeloid precursor 32Dcl3 (32D) cells, in which apoptosis was blocked by zVADfmk (Supplementary Figure 7A, B). Moreover, a net increase in the conversion of LC3-I to LC3-II was also readily detected upon IL-3 withdrawal (Supplementary Figure 7C).

IM induces autophagy in p210$^{BCR/ABL}$-expressing 32D cells

To confirm the link between inhibition of BCR/ABL tyrosine kinase and induction of autophagy, we analyzed endogenous levels of LC3 in IM-treated p210$^{BCR/ABL}$ – expressing 32D cells. Indeed, IM (1 μM) induced autophagy, as demonstrated by the presence of large LC3-positive vacuoles in the cytoplasm (Figure 2A). Moreover, Western blot analysis revealed the accumulation of LC3-II in protein extracts of treated cells (Figure 2B).

To assess whether induction of autophagy was due to sudden lack of survival signals following BCR/ABL inhibition, IL-3-independent eGFP-LC3-transduced 32D-p210$^{BCR/ABL}$ cells were treated with 1μM IM, alone or in the presence of 0.5-5ng/ml IL-3 (Figure 2C). The presence of IL-3 in the culture media significantly impaired the accumulation of LC3-II (Figure 2C), suggesting that the autophagic response is connected to the IM-dependent ablation of intracellular survival signals. Yet, autophagy induction could be a non-specific consequence of IM treatment. To exclude this, we analyzed the effects of IM on eGFP-LC3-transduced 32D-v-Src cells; in these cells, treatment with IM failed to induce accumulation of eGFP-LC3 (Figure 2D). Likewise, IM did not induce autophagy in eGFP-LC3-expressing HeLa cells (Supplementary Figure 8). Finally, we tested whether IM-dependent induction of autophagy was due only to inhibition of p210$^{BCR/ABL}$. First, eGFP-LC3-transduced 32D cells expressing the IM-resistant T315I p210$^{BCR/ABL}$ mutant (32D-T315Ip210$^{BCR/ABL}$) did not show LC3 processing upon IM treatment (Figure 2E). Second, ectopic expression of the IM-resistant T315I c-Abl mutant in 32D-p210$^{BCR/ABL}$ cells did not block IM-induced autophagy, demonstrating that the effect is BCR/ABL-dependent (Figure 2F).

IM-induced autophagy is preceded by ER stress and relies on intracellular calcium

Several studies have implicated ER stress in the induction of autophagy through the activation of different downstream pathways ((47) and references cited therein). Furthermore, inhibition of c-Abl by IM induces ER stress in cardiomyocytes (50). Therefore, we hypothesized that IM could cause ER-stress also in BCR/ABL-expressing cells and this could be involved in the induction of autophagy. To address this possibility, 32D-p210$^{BCR/ABL}$ cells were treated with or without 1μM IM and the mRNA levels of C/EBP homologous protein (CHOP), a marker of the ER-stress response activated by transcriptional mechanisms, were measured by real-time quantitative PCR. We found a significant increase in CHOP mRNA levels (P=0.004) as early as one hour after IM treatment (Figure 3A). Expression of Grp78, another marker of the ER stress response (51), was also rapidly induced in IM-treated cells (Figure 3B). Up-regulation of both markers preceded the induction of autophagy, as LC3 conversion was detected only 3 hours after IM treatment (not shown). Cellular

calcium homeostasis has been reported to be perturbed by ER stress and to be causally linked to the induction of autophagy (52, 53). Consistent with this, treatment of 32D-p210$^{BCR/ABL}$ cells with 2μM IM produced a marked reduction in the ER Ca^{2+} pool as defined by thapsigargin-mediated Ca^{2+} release (Figure 3C and 3D). To assess calcium requirements in IM-induced autophagy, eGFP-LC3-transduced K562 and 32D-p210$^{BCR/ABL}$ cells were treated with 1μM IM alone or in combination with 5mM ethylene glycol tetraacetic acid (EGTA) or 10μM bis-(0-aminophenoxy)-ethane-N,N,N,N'-tetraacetic acid/tetra (acetoxymethyl)-ester (Bapta/AM) to chelate extracellular and intracellular Ca^{2+}, respectively. Remarkably, IM-dependent conversion of LC3 was totally abrogated when cytosolic calcium was depleted using Bapta/AM (Figure 3E and 3F). By contrast, EGTA did not alter IM-dependent accumulation of LC3-II, implying that only calcium derived from intracellular stores, such as ER, accounted for the induction of autophagy (Figure 3E, F).

Inhibition of autophagy potentiates IM-induced cell death in p210$^{BCR/ABL}$-expressing 32D cells

Several studies have suggested that autophagy may act as a protective mechanism in tumor cells (32, 33, 36, 37) and that therapy-induced cell death can be enhanced upon autophagy inhibition (38-42). To test whether autophagy acts as a survival mechanism in our system, we inhibited autophagy in 32D-p210$^{BCR/ABL}$ cells using CQ and analyzed the effects on IM-induced cell death. While treatment with CQ alone had no effect, IM-induced cell death was significantly increased (from 50 to over 75%; P= 0.024) when IM was combined with CQ (Figure 4A). Similar results were obtained using Bafilomycin A1 (Ba), an inhibitor of autophagy that acts by blocking the activity of the H^+-ATPase responsible for acidification of autophagolysosomes, or 3-methyladenine, an inhibitor which blocks the early stages of autophagy (28, 29) (Figure 4B and not shown). In contrast, 32D cells expressing the IM-resistant T315I p210$^{BCR/ABL}$ mutant (32D-T315Ip210$^{BCR/ABL}$), which do not undergo autophagy upon IM treatment (Figure 2E), were not sensitive to CQ treatment (Figure 4C).

We also assessed whether treatment with CQ would potentiate the effects of IM in mice inoculated with 32D-p210$^{BCR/ABL}$ cells. Thus, sublethally-irradiated C3H/HeJ mice were injected intravenously with LC3-GFP 32D-p210$^{BCR/ABL}$ cells (2.5

x 10^5/mouse) and divided in four groups: i) untreated mice; ii) mice treated with CQ only; iii) mice treated with IM only: and iv) mice treated with IM and CQ.

Leukemia was allowed to develop and 14 days post-injection when GFP-positive cells in the bone marrow were typically 30-40%, mice were treated with IM (100mg/Kg/5 consecutive days), CQ (60mg/mouse, 7 intraperitoneal injections) or the IM/CQ combination. In the IM/CQ-treated group, mice were pre-treated for 2 days with CQ before starting the therapy with IM. 24 hours after the end of the treatment, mice (3/group) were sacrificed and GFP-positive cells assessed in the bone marrow. GFP-positive cells in untreated and CQ-treated mice were 60 ± 12% and 50 ± 6.8%, respectively; as expected, IM treatment induced a decrease in the number of bone marrow GFP–positive cells (33.0 ± 10%); this decrease was more pronounced in the mice treated with IM and CQ (10.6 ± 7.8 % GFP positivity) (Figure 5A).

The viability of GFP-positive cells in the bone marrow was evaluated by methylcellulose colony formation (CFC) assays in the absence of cytokines. On plating an equal number of cells (1,000/plate), a similar number of colonies formed from bone marrow of untreated and CQ-treated mice; less colonies grew from marrow of mice treated with IM only and even fewer colonies formed from marrow of mice treated with the IM/CQ combination (Figure 5B).

Next, we investigated the type of cell death induced by CQ-mediated sensitization, and specifically whether caspase-dependent or -independent mechanisms were involved. To this end, 32D-p210$^{BCR/ABL}$ cells were treated with 1μM IM along with 5μM CQ and 50μM zVADfmk and the percentage of annexin V-positive cells was determined (Figure 4D). At the same time, caspase activity was measured in protein extracts using a DVED fluorescent substrate (Figure 4D). We found that CQ-mediated sensitization did not require caspase activation, as the combination of IM and CQ significantly augmented cell death in cells treated with zVADfmk to block caspase activity (Figure 4D). However, IM-induced cell death was reduced in cells treated with zVADfmk, consistent with the ability of BCR/ABL proteins to block caspase 3 activation (54). Next, we tested whether inhibition of the intrinsic apoptotic pathway would have any effect on CQ-mediated sensitization. 32D-p210$^{BCR/ABL}$ cells stably overexpressing Bcl-2 (55) and retrovirally transduced with MigRI-eGFP-LC3 were treated with 1 or 2μM IM in the presence or absence of CQ, and analyzed for induction of cell death at different time points (Figure 4E).

While Bcl-2 overexpression delayed IM-induced cell death, it did not make cells refractory to CQ-mediated sensitization, which was even higher than in parental 32D-p210$^{BCR/ABL}$ cells (compare Figure 4A and 4E). GFP-LC3-II was readily detected as early as 6 hours after IM treatment of Bcl-2-expressing 32D-p210$^{BCR/ABL}$ cells (Figure 4F), indicating that in these cells Bcl-2 over-expression does not block autophagy, at variance with what has been suggested by previous reports in other models (32, 56).

Inhibition of autophagy increases IM-induced cell death in cell lines and primary CML cells

As CQ potentiates IM-induced cell death in 32D-p210$^{BCR/ABL}$ cells, we performed experiments to determine if inhibition of autophagy leads to increased cell death in IM-treated CML cell lines. These studies were carried out by use of chemical inhibitors and by si/shRNA-dependent ablation of the expression of essential autophagy genes. The combination of IM and CQ treatment significantly augmented cell death in K562 cells compared to IM alone (P=0.015) (Figure 6A). Bafilomycin A1 also enhanced IM-induced cell death, demonstrating that the potentiating effect is not limited to CQ (Figure 6B). To assess whether CQ affects survival in long-term assays, we performed CFC assays using K562 cells treated with 0.25 or 0.5μM IM. CQ enhanced the effect of IM at 0.5μM even more potently than in the short-term survival assay (compare Figure 6A and Figure 6C). CQ treatment of a sub-clone of K562 cells resistant to IM as a consequence of gene amplification (57) also enhanced the survival- inhibitory effects of IM (Figure 6D). Finally, CQ treatment increased cell death in IM-treated BV173 cells, and the sensitizing role of autophagy inhibition was also confirmed using Bafilomycin A1 (Supplementary Figure 9A, B).

Since CQ and Bafilomycin A1 could enhance IM-induced cell death by mechanisms independent of their effects on autophagy (i.e. non-specific effects), we knocked down expression of the essential autophagy genes ATG5 and ATG7 in K562 cells using specific siRNAs and analysed whether autophagy was blocked and cells sensitized to IM-induced cell death. Indeed, down-regulation of ATG5 or ATG7 expression blocked the IM-induced accumulation of the LC3-II isoform and enhanced the cell death-inducing effect of IM (Figures 6E-H). Finally, in K562 cells transduced with pGIPZ lentiviral vectors expressing a scrambled shRNA (SO) or an ATG7-specific shRNA, stable downregulation of ATG7 expression (Figure 6I, upper

panel) blocked IM-induced LC3-II accumulation (Figure 6I, lower panel) and promoted an increase in IM-induced cell death (Figure 6K).

We next investigated whether IM treatment induced autophagy in primary CML cells and whether inhibition of autophagy enhanced the cell death-inducing effect of IM in these cells. Peripheral blood CD34+ cells from a partially IM-resistant (M351T) CML patient were left untreated or treated with IM (2μM) for 24 hours and assessed for induction of autophagy by detection of the autophagic LC3-II isoform. Anti-LC3 Western blotting of protein extracts from CML cells showed a clear accumulation of LC3-II and an increase (approximately 10-fold) of the LC3-II/LC3-I ratio in IM-treated cells (Figure 7A).

To assess whether IM-induced autophagy provided a survival advantage to these cells, CFC assays were performed after a 24 hour treatment with IM, CQ or the IM/CQ combination. Treatment with CQ (10μM) or IM (0.5μM) alone had a modest effect on colony formation of these cells; by contrast, fewer colonies formed after treatment with 1.0μM IM and there was an additional 60% decrease upon treatment with the IM/CQ combination (Figure 7B). Finally, to determine whether genetic ablation of autophagy had similar effects on colony formation, we employed RNA interference of ATG5 or ATG7 to suppress autophagy in primary CML cells with the M351T mutation. Remarkably, knockdown of ATG5 or ATG7 expression (Figure 7D) enhanced the colony formation inhibitory effect of IM (Figure 7C).

CFC assays were also performed upon IM, CQ and IM/CQ treatment of peripheral blood mononuclear cells from newly diagnosed CML-CP patients. Colony number was decreased in the presence of IM/CQ compared to IM alone (Supplementary Figure 10A-D). Comparable results were obtained with two additional CML samples (not shown). We next analyzed colony formation of mononuclear CML cells (70% CD34+) from a relapsed CML patient carrying the partially IM-resistant V299L $p210^{BCR/ABL}$ mutant (20). Like the CML sample with the M351T mutation (Figure 7B), CML cells became more sensitive to low doses of IM upon co-treatment with CQ (Supplementary Figure 10E). In contrast, normal marrow mononuclear (n=3) or peripheral blood CD34+ cells (n=2) did not show a further decrease in colony formation when treated with the IM/CQ combination (Supplementary Figure 10F, G) demonstrating that the effect of the combination was specific for $p210^{BCR/ABL}$-expressing cells.

Similar results were obtained using cells from a newly diagnosed CML-CP patient that had just started IM treatment (3 days at 800mg/day; CML-CP-t-1; Supplementary Figure 11A) and a CML-CP patient undergoing IM treatment (10 days at 100mg/day; CML-CP-t-2; Supplementary Figure 11B; low IM doses were used due to development of bone marrow aplasia). Interestingly, CQ alone markedly suppressed colony formation of CML cells from patient CML-CP-t-1, suggesting that high-dose IM treatment was particularly effective in sensitizing CML cells to CQ, probably because of induction of autophagy in vivo. Indeed, LC3-positive vacuoles were readily detected in peripheral blood mononuclear cells of both patients (not shown).

Tyrosine kinase inhibitor treatment in combination with inhibition of autophagy results in near complete eradication of CML stem cells

Previous studies have shown that in vitro treatment with TKI does not eradicate CML stem cells (23-27). To determine whether TKI-induced autophagy is a potential survival mechanism for this cell population, colony forming cell (CFC) and long term culture-initiating cell (LTC-IC) assays were performed. For CFC assays, CP-CML cells (n=6) were first sorted into primitive (CD34+CD38-) and more mature progenitor (CD34+CD38+) populations and were left untreated or pre-treated for 48 hours with TKI (IM, nilotinib or Das) or autophagy inhibitor (CQ, Ba) alone, or the TKI/CQ/Ba combination in SFM supplemented with five growth factor (5GF) cocktail.. The number of CFC obtained for each sample was then compared to a baseline – cells which had no prior culture or treatment (100%). Notably, treatment with IM (2 μM) and Das (150 nM) induced accumulation of LC3-positive vesicles in primitive progenitor cells (Figure 8A). As shown in Figure 8B for the CD34+CD38+ population, the untreated cells showed a doubling of CFC over the 48 hours "pre-treatment", consistent with stem/progenitor cell expansion in the culture medium. Neither CQ nor Ba alone had any effect on this expansion. However, as shown previously (19, 24) the TKI IM, Das (10nM) and nilotinib, all exhibited an anti-proliferative effect which prevented any CFC expansion over baseline. Dasatinib, at the highest clinically achievable concentration (150nM), was able to reduce the number of CFC to 55% of baseline, suggesting some level of apoptosis. This effect was dramatically increased following TKI/autophagy inhibitor combination treatment,

with 80-95% reduction in colony formation versus baseline and even more impressive compared to the no drug control (Figure 8B). For CD34+CD38- cells (Figure 8C), that are consistently resistant to TKI, treatment with TKI/autophagy inhibitor was extremely effective with only 2% CFC remaining following Das (150nM)/CQ exposure.

Since the CFC assay measures a relatively mature, committed progenitor cell population, LTC-IC assays were also carried out to measure the effect of autophagy inhibition on the functionality of more primitive CML cells. As the presence of cytokines in the culture media may alter the requirement of autophagy for cell survival, the LTC-IC assays were carried out both in the presence and absence of a 5GF cocktail. CP-CML CD34= cells (n=3) were left untreated or pre-treated for 6 days with TKI (IM or Das) or CQ alone, or the TKI/CQ combination. As with the CFC assay, the number of LTC-IC obtained for each sample was then compared to a baseline. With 5GF, untreated and CQ-treated cells formed 67 and 47% less colonies than cells at baseline, respectively, suggesting that a large proportion of these cells has proceeded towards terminal differentiation (Figure 8D). Consistent with the CFC data and previous studies (24), treatment with IM or Das was antiproliferative even in the presence of 5GF and therefore resulted in a protective effect on the number of LTC-IC over baseline. Combination treatment with TKI and autophagy inhibition counteracted this protective effect and resulted in an impressive decrease in the number of LTC-IC, with a significant reduction for IM/CQ and Das/CQ versus TKI alone (approximately 4.5 and 6-fold, respectively) (Figure 8D). Untreated and CQ-treated cells cultured without supplemental GFs formed reduced numbers of colonies, as compared to baseline cells (Figure 8E). The removal of GFs combined with TKI treatment had a dramatic effect on the number of LTC-IC obtained (6.5% and 4.1% for IM and Das, respectively), suggesting that cytokines may play an important protective role for the survival of TKI-treated CML cells, consistent with the results of a previous study (58). Combination treatment with CQ resulted in an even greater in LTC-IC numbers (1% and 0.6% for IM/CQ and Das/CQ, respectively), indicating that BCR/ABL inhibition via TKI treatment combined with autophagy inhibition of GF-starved CML promotes the most effective elimination of primitive CML cells.

Discussion

IM has revolutionized the therapy of CML, as most patients in the CP of the disease undergo durable remission when treated with this drug on a continuous basis. However, development of resistance and the limited efficacy of IM in CML-BC patients represent shortcomings of the therapy. In more than 40% of cases, resistance is the result of mutations inside and around the kinase domain of BCR/ABL that impair IM binding (14-18). Resistance also occurs through overexpression of BCR/ABL or gene amplification (59), involvement of glycoproteins (60), activation of Lyn kinase (61-63) and other mechanisms. To address this problem, new TKI such as the dual Src/BCR/ABL inhibitor Das, were developed (64, 65). However, Das treatment is also ineffective in CML patients carrying the BCR/ABL T315I mutation that prevents IM binding to the kinase domain (65). Although more potent and specific BCR/ABL inhibitors are being developed and tested in clinical trials, an on-going problem with this approach is the selection of additional mutations causing drug resistance in patients (66). In CML patients in CP who are responding optimally to IM therapy minimal residual disease is detectable using highly sensitive quantitative PCR, suggesting that the most primitive cells are not eradicated by TKI. We have previously demonstrated that CML stem cells overexpress p210BCR/ABL and are inherently resistant to IM, Das, nilotinib and bosutinib (24-27). For these reasons, alternative approaches that combine a TKI with a second agent exhibiting a different mechanism of action are required if we are to improve CML therapy.

One of the most evident effects of IM on CML cells is induction of cell death due to insufficient survival signals following BCR/ABL inhibition. However, it is still unclear whether IM affects other cellular functions. We reasoned that it would be important to evaluate additional intracellular changes induced by IM treatment and to investigate whether some of the changes could be exploited for therapeutic intervention. We show here that cell shrinkage is one of the more evident effects of IM treatment in the CML cell lines K562 and BV173. This occurs in viable cells and is characterized by reduction of cytoplasmic content and accumulation of vacuoles, a phenomenon reminiscent of cell atrophy following growth factor deprivation-induced autophagy in myeloid cells (33). Indeed, IM treatment of BCR/ABL-expressing cell lines and primary cells induced morphological and biochemical hallmarks of autophagy such as generation of autophagosomes, LC3-positive autophagy-like

vacuoles and LC3-II accumulation. In the BV173 line, vacuoles were only evident upon treatment with CQ, which blocks degradation inside autophagolysosomes, suggesting that high lysosomal activity was responsible for the efficient turnover of LC3 and its associated vacuoles. By contrast, IM did not cause autophagy in v-Src-transformed 32D cells, IM-resistant 32D-$p210^{BCR/ABL}$ cells and HeLa cells. Expression of an IM-resistant c-Abl mutant did not inhibit induction of autophagy in 32D-$p210^{BCR/ABL}$ cells, clearly demonstrating that the effect of the drug is specific and occurs predominantly through inhibition of BCR/ABL. Overall, these findings suggest that a sudden decrease of survival signals, triggered by inhibition of the $p210^{BCR/ABL}$ tyrosine kinase, induces the rapid activation of an autophagy program.

We next focused on the potential pathways involved in IM-dependent induction of autophagy. Recent studies have shown that ER stress can trigger autophagy by several mechanisms (52, 53). Interestingly, BCR/ABL has been shown to regulate ER calcium homeostasis and inhibit ER stress-induced cell death (67). Therefore, it is conceivable that inhibition of $p210^{BCR/ABL}$ could affect ER function. Indeed, IM rapidly induced expression of the ER stress markers CHOP and Grp78, and this preceded the accumulation of LC3-II, suggesting that ER stress is implicated in IM-triggered autophagy. Interestingly, calcium was released from the ER following IM treatment and was required for autophagy induction. Together, these data suggest that induction of ER stress upon BCR/ABL inhibition may cause autophagy. ER stress has been reported to trigger autophagy through inhibition of mTOR (52, 53). Consistent with this, treatment of K562 cells with the mTOR inhibitor, rapamycin, induced the conversion of LC3-I into the autophagosome-associated LC3-II (data not shown).

What would the role of autophagy be in IM-treated $p210^{BCR/ABL}$-expressing cells? We hypothesize that autophagy represents a condition upon which BCR/ABL-transformed cells rely to reach a state of metabolic inertia following cessation of anti-apoptotic signals. Therefore, autophagy would represent a survival mechanism. To directly test this, we assessed whether IM-induced cell death would be enhanced by chemical and genetic inhibition of autophagy using CQ to inhibit the last step of the autophagic process (i.e. the degradation of autophagosomes following fusion with lysosomes (34)) and RNAi of essential autophagy genes. Remarkably, CQ treatment potentiates IM-induced cell death. However, this effect is abrogated in cells expressing the IM-resistant T315I $p210^{BCR/ABL}$ mutant, but is not affected by

expression of the IM-resistant T315I c-Abl mutant (not shown). This confirms that inhibition of BCR/ABL is the main trigger of autophagy. CQ also has a sensitizing effect on IL-3-deprived parental 32D cells undergoing autophagy (not shown), again supporting the notion that BCR/ABL inhibition mimics growth factor deprivation and that in this context autophagy is a protective mechanism. CQ-dependent potentiation of IM-induced cell death (by annexin V staining and clonogenic assays) is also evident in BV173 and K562 cells, including a partially IM-resistant K562 sub-line. Inhibition of autophagy by RNAi-mediated knockdown of either ATG5 or ATG7 resulted in comparable sensitizing effects, demonstrating that the effects of CQ and Bafilomycin A1 depend, to a large extent, on suppression of autophagy. A recent study suggested that the cell death-promoting effect of CQ in a model of Myc-induced lymphomagenesis is p53-dependent (34); this mechanism clearly does not explain the effect of CQ (or Bafilomycin A1) in the p53-null K562 cells (68). Since p53 is mutated in approximately 25% of CML-BC patients (69, 70), it would be attractive to be able to enhance the therapeutic effects of TKI via p53-independent mechanisms. Remarkably, the IM/CQ combination is effective in primary CML cells and also in cells carrying partially IM-resistant $p210^{BCR/ABL}$ mutants, while normal mononuclear and CD34+ cells were much less affected. Treatment with CQ alone had some inhibitory effect on colony formation of CML mononuclear cells and, to a lesser degree, of the normal counterpart. Whether this reflects a baseline level of autophagy in normal and CML late myeloid progenitor/precursors it is unclear; however, early progenitors from healthy donors and CML patients were almost completely insensitive to treatment with CQ alone, suggesting that CQ toxicity to normal marrow progenitors may not be a concern in CML patients treated with the TKI/CQ combination.

To date TKI used as single agents have been ineffective in killing primitive CML cells (22-27). Recently, we demonstrated that the combination of a TKI with the farnesyl transferase inhibitor, BMS-214662, resulted in potent, selective eradication of CML stem cells, including functionally defined CFC and LTC-IC (24). Importantly, we show here that these cells undergo autophagy upon TKI treatment and are highly susceptible to killing by the combination of TKI and inhibition of autophagy. These data are extremely encouraging and suggest it will be possible to target the cancer stem cell population in a selective manner without compromising the survival of normal stem cells. Finally, cells isolated from CML-CP responsive to IM

treatment appear to be particularly sensitive to treatment with CQ alone, suggesting that IM treatment can induce autophagy *in vivo*.

Overall, our findings clearly demonstrate that: i) autophagy acts as a survival signal in $p210^{BCR/ABL}$-expressing cells treated with TKI; ii) its inhibition can be exploited to potentiate TKI-induced cell death, raising the possibility that the combination of IM and CQ, or more clinically applicable inhibitors of autophagy, may be beneficial in the treatment of CML (Figure 9), and iii) that such a combination can target the TKI-resistant CML stem cell population**.** Consistent with the concept that induction of autophagy provides a survival mechanism to IM-treated CML cells , a recent report has proposed that resistance of CML cells to histone deacetylase inhibitors can be reverted by using autophagy inhibitors (71).

More generally, our work reinforces the notion that cancer cells, including cancer stem cells, can survive in a stressful environment, following inhibition of critical oncogenic pathways, by inducing autophagy. These tumor cells are primed to resume proliferation under more favourable conditions e.g. if drug concentrations drop below a certain threshold due perhaps to drug withdrawal related to toxicity or non-compliance or following development of mutations that promote drug resistance.

Thus, future therapeutic strategies that aim to inhibit autophagy in cancer cells treated with conventional chemotherapy or novel small molecules, including TKI, represent a promising approach that will target both bulk tumor and cancer stem cells.

Experimental procedures

Reagents

IM and nilotinib were obtained from Novartis Pharma. A 100mM stock solution of IM in sterile distilled water was stored at 4°C. A 10mM stock solution of nilotinib in dimethyl sulfoxide (Sigma-Aldrich, St Louis, MO) was stored at -20°C. Das was purchased from LC Laboratories (Woburn, MA, USA). Stock solutions of 10mg/mL were stored at -20°C. Dilutions of these drugs in phosphate-buffered saline (PBS) were freshly prepared for each experiment.

Cell cultures

BV173 and K562 cells were cultured in Roswell Park Memorial Institute (RPMI) medium supplemented with L-glutamine, 10% fetal bovine serum (FBS, Hyclone) and penicillin/streptomycin. All other hematopoietic cell lines (32D and derivatives) used in this study were cultured in Iscove's Modified Dulbecco's Medium (IMDM) with L-glutamine and supplemented with 10% FBS and penicillin/streptomycin. CML cells were obtained from newly diagnosed or relapsed patients after informed consent according to institutional guidelines. Mononuclear cells were obtained by centrifugation on a Ficoll-Hypaque gradient (Amersham Biosciences, Uppsala, Sweden) while CD34+ cells were FACS-sorted with the PE-conjugated anti-human CD34 antibody (clone 563, BD Pharmingen). Presence of mutations in the kinase domain was assessed by sequencing. Normal marrow mononuclear cells were obtained from healthy donors. Peripheral blood (G-CSF-mobilized) normal CD34+ cells were purchased from StemCell Technologies (Vancouver, Canada). Cells were cultured in StemSpan SFEM medium (StemCell Technologies) supplemented with cytokine cocktail (STEMSPAN CC100, StemCell Technologies) containing Flt-3 ligand (100ng/ml), KL (100ng/ml), IL-3 (20ng/ml), IL-6 (20ng/ml). HeLa cells were cultured in Dulbecco's modified Eagle's medium supplemented with 10% FBS and penicillin/streptomycin. Cells were maintained in a Heraeus CO_2 Auto-Zero incubator at 37°C with 5% CO_2. All reagents were purchased from GIBCO, unless otherwise stated.

Isolation of CD34+CD38+ and CD34+CD38- cells

Fresh leukapheresis or peripheral blood samples were obtained with written informed consent from patients with newly diagnosed CML in CP (n=6). Samples were enriched for CD34+ cells using CliniMACS (Miltenyi Biotec, Auburn, CA) according to the manufacturer's instructions and cryopreserved in 10% (v/v) dimethyl sulfoxide in ALBA (4% [w/v] Human Albumin Solution, Scottish National Blood Transfusion Service). Purity of CML CD34+ cells was more than 95% and > 95% were Ph^1as assessed by D-FISH. CD34+ CML cells were simultaneously stained with CD34-APC and CD38-FITC (BD Biosciences, San Jose, CA) and sorted to isolate the CD34+ and the CD34+38- subpopulations using a FACSAria (BD Biosciences). Cells were then cultured in Iscove's Modified Dulbecco's Medium (Sigma-Aldrich) supplemented with a serum substitute (BIT; StemCell Technologies, Vancouver, Canada), 10 mg/ml LDL, 0.1μM 2-mercaptoethanol (Sigma), 1% glutamine (100mM, Invitrogen, Paisley, UK) and 1% penicillin-streptomycin (100mM, Invitrogen) (Serum Free Medium, SFM). SFM was further supplemented with a a 5GF cocktail comprising 100ng/mL Flt3-ligand and 100ng/mL Kit ligand and 20ng/mL each of IL-3, IL-6 (StemCell Technologies) and G-CSF (Chugai Pharma Europe Ltd, London,UK), as indicated.

Colony forming assays

K562, primary CML cells, normal marrow mononuclear cells and peripheral blood CD34+ cells were treated for 24 hours with the indicated concentrations of CQ or IM, individually or in combination. Drug-treated cells were seeded in Methocult H4230 methylcellulose medium (StemCell Technologies) in the absence of cytokines (K562 cells) or in the presence of a cytokine cocktail (STEMSPAN CC100, StemCell Technologies) containing Flt-3 ligand (100ng/ml), KL (100ng/ml), IL-3 (20ng/ml), IL-6 (20ng/ml) (CML, marrow mononuclear and CD34+ cells) with the indicated concentrations of CQ or IM. Formation of colonies was assessed 7 days after plating 1,000 (K562), 2,500 (normal CD34+) or 25,000-50,000 (normal mononuclear and primary CML) cells/plate. CD34+CD38+ and CD34+CD38- CML-CP cells were pre-treated for 48 hours with the indicated concentrations of IM, Das, nilotinib, CQ and Ba, either alone or in combination. Untreated, drug-treated and cells which had no prior culture or treatment (baseline) were seeded in Methocult methylcellulose

medium (StemCell Technologies), in the presence of indicated drug concentrations (from pre-treatment). Formation of colonies was assessed 14 days after plating 10,000 cells/plate.

LTC-IC assays

M2-10B4 cells and S1/S1 fibroblasts were first established as feeder layers and then irradiated at 80Gy. CML-CP CD34+ were pre-treated with or without 5GF for 6 days with IM (2µM), Das (150nM), and CQ (10µM), alone or in combination. All CML cells remaining after culture were washed twice to remove drugs and then untreated, drug-treated and cells which had no prior culture or treatment (baseline) were plated in duplicated on the irradiated feeders in Myelocult medium (StemCell Technologies). Cultures were maintained for 5 weeks with weekly half medium changes. After 5 weeks, cell counts were performed and 1 x 10^5/ml cells were transferred to CFC assays and maintained in culture for an additional 2 weeks in Methocult (StemCell Technologies) before the colonies were scored.

Treatment of leukemic mice with IM, CQ or the IM/CQ combination

Sub-lethally-irradiated C3H/HeJ mice were injected intravenously with MigRI GFP-LC3-transduced 32D-p210$^{BCR/ABL}$ cells (2.5x10^5 cells/mouse) and divided into four groups (untreated, treated with IM only, CQ only, or the IM/CQ combination). For IM only treatment, mice were treated with 100mg/Kg/day for 5 consecutive days (by gavage) starting 14 days post-injection of leukemic cells; for CQ only treatment, mice were treated with 60mg/Kg/ day for 7 consecutive days (by intraperitoneal injection) starting 12 days post-injection of leukemic cells; for the IM/CQ combination treatment, mice were pre-treated with CQ (60mg/Kg/mouse) for 2 days (starting at day 12 post-injection of leukemic cells) and on day 14 treated with IM and CQ at the dose and schedule indicated above for single treatments. Untreated and treated mice were sacrificed 20 days post-injection of LC3-GFP 32D-p210$^{BCR/ABL}$ cells.

Fluorimetric assay of caspase activity

Activity of the effector caspases 3 and 7 in cell lysates was assessed by the cleavage of DEVD.AFC (72) and measured (excitation/emission = 405/510 nm) at 37°C in 96-well plates in 200µl of assay buffer (20µM Z-DEVD.AFC, 0.1% CHAPS, 10mM dithiothreitol, 100mM HEPES, and 10% sucrose, pH 7.0) using a Wallac Victor2

1420 Multilabel counter. The 96-well plates were assayed for 10 cycles, and cleavage rates were determined by linear regression. The protease activities were expressed as pmol/min/mg protein.

Quantification of calcium content in the ER

$P210^{BCR/ABL}$ 32D cells were incubated with 2μM IM in cell culture medium (see above). For the last 45 min, cells were additionally incubated with the fluorescent Ca^{2+} indicator Fura-2 AM. At the end of this time period, cells were pelleted and then resuspended in a Ca^{2+}-free Krebs-Henseleit buffer (in mM: NaCl 118, KCl 4.7, $MgSO_4$ 1.2, KH_2PO_4 1.2, $NaHCO_3$ 4.2, HEPES 10, glucose 11.7, pH 7.4). The cell suspension was placed in a UV grade cuvette and intracellular Ca^{2+} measure in a PerkinElmer LS55 fluorimeter. Cells were stirred continuously and maintained at 37°C. The content of the ER Ca^{2+} pool was estimated from the magnitude of Ca^{2+} rise evoked by addition of the SERCA pump inhibitor thapsigargin (5μM).

Retroviral infection

For retroviral infection, Phoenix cells (kind gift of G.P. Nolan, Stanford University School of Medicine, Stanford, CA) were transiently transfected with the indicated plasmids. The infectious supernatant was collected 24 hours later and used for infection. Twenty-four hours later, infected cells were sorted (EPICS profile Analyzer, Coulter, Hialeah,FL) for GFP expression.

Determination of autophagy

Autophagy was assessed in cells cultured in the presence or absence of IM by measuring levels of cytosolic LC3-I and autophagosomes-associated LC3-II. Briefly, cells were plated at a density of 1×10^5 cells/ml unless otherwise stated. Cells were cultured in the presence of 1 to 4μM IM and harvested 6 or 12 hours later. The effect of calcium on IM-dependent autophagy was assessed by culturing the cells in the presence or absence of 5mM EGTA (Sigma) and/or 10μM Bapta/AM (Calbiochem) for 6 or 12 hours. 3.5×10^5 cells were harvested, rinsed twice with cold PBS (Sigma) and lysed directly in Laemmli's sample buffer supplemented with β-mercaptoethanol (Sigma). Finally, protein extracts were subjected to SDS-PAGE and analyzed by standard Western blotting. HeLa cells stably expressing eGFP-LC3 were seeded at

1.5×10^5/ml in a 6-well plate and left adhering overnight. The following day, media was replaced and cells were cultured in the presence or absence of 1 and 5μM IM for 6 or 12 hours. Cells were then harvested, and protein levels were measured. Primary antibodies used were: anti-LC3 (Sigma) and anti-Actin (Sigma). To assess expression of Grp78, cells were cultured in the presence of 2μM IM and harvested 1, 3 and 6 hours later. Grp78 was detected using anti-BiP/Grp78 monoclonal antibody (BD Transduction Laboratories). Anti-rabbit and –mouse horseradish peroxidase-conjugated secondary antibodies were purchased from Amersham and ECL solution from Pierce.

Immunohistochemistry

Morphological analysis was performed by standard May-Grunwald/Giemsa staining as described (73). In brief, cells were cytospun on top on poly-L-lysine coated microscope slides (Menzel) at 200rpm for 5 min using a cytocentrifuge (Shandon). Slides were dried for 30 min at room temperature, stained for 3 min with a May-Grunwald solution (Sigma) and rinsed with an excess of bidistilled H_2O for 1 min. Then, nuclei were counterstained for 30 min using a Giemsa solution (Sigma) and rinsed as described above. Slides were analyzed using an Axiostar direct light microscope (Zeiss) and pictures of cells were acquired using a ProgRes C-14 RGB camera.

Immunofluorescence

Immunofluorescence was performed as described (74) with some modifications. Briefly, 5×10^4 cells were cytospun on poly-L-lysine coated microscope slides (Menzel) at 200rpm for 5 min by using a cytocentrifuge (Shandon). Slides were dried for 30 min, fixed with 4% paraformaldehyde (Sigma), permeabilized with 0.1% Triton-X 100 (Sigma) for 3 min and incubated with a primary antibody for 1 hour. FITC- or TRITC-conjugated secondary anti-mouse antibodies used in this study were purchased from Molecular Probes. Finally, nuclei were counterstained by Hoechst (Sigma) and slides were analyzed using a laser scanning confocal microscope (LSM 510 Zeiss system). Primary antibody used in this study was anti-LC3 (Nanotools).

Quantification of cell death

Apoptosis was quantified by phosphatidylserine externalization in the presence of propidium iodide (PI) as described (75). In brief, cells were cultured in the presence of 1 or 2μM IM, alone or in combination with 5μM CQ for 12 and 48 hours. Cells were stained with allophycocyanin conjugated (APC)- annexin V (Molecular Probes, Invitrogen), PI (Sigma) and analyzed using a FACSCalibur system (Becton Dickinson). Data were expressed as mean ± SEM of three independent experiments, analyzed by unpaired *t*-test (Graphpad Software, Inc, San Diego, CA) and *P* values less than 0.05 were considered statistically significant.

Electron microscopy and immunogold cytochemistry

Cells were fixed with 2% glutaraldehyde in 0.1M sodium cacodylate buffer, pH7.4, postfixed with 1% osmium tetroxide/1% potassium ferrocyanide, en bloc- stained with 5% uranyl acetate, and embedded in Taab epoxy resin (Taab Ltd., UK). Duplicate pellets were fixed with 4% formaldehyde, freshly made from paraformaldehyde in Dulbecco's PBS, pH7.4, for 1 hour at room temperature. These cells were embedded in LR-White resin (Agar Scientific, Stansted, UK); ultra-thin sections were incubated with the anti-GFP antibody and labeled with immunogold (British Biocell International, Cardiff, UK). Control incubations involved the replacement of primary antibody with an equivalent concentration of an isotype-specific IgG. All sections were examined unstained or after staining with lead citrate and/or uranyl acetate.

RNA interference

For siRNA transfection we used the Amaxa cell nucleofection kit V. Cells ($1x10^6$) were resuspended in 100μl of nuclefector V solution and cell suspensions were mixed with 5μg of siRNA. The solution was added to the Amaxa electrode cuvettes and electroporated in Amaxa Electroporetor II, using program T-16 for K562 and U-08 for CD34+ CML cells, respectively. Immediately afterward, cells were diluted in 2mL IMDM (supplemented with 10% FBS, 100U/ml penicillin, 0.1mg/ml streptomycin, 2mM L-glutamine) at 37^oC ($5x10^5$ cells/ml). The siRNA corresponding to the human cDNA sequence for ATG5 (5'-GCAACTCTGGATGGGATTG-3') and ATG7 (5'-CAGTGGATCTAAATCTCAAACTGAT-3') were synthesized by Sigma-Aldrich

and Ambion/Applied Biosystems. Control siRNAs were purchased from Ambion. Downregulation of ATG5 and ATG7 expression was verified by western blotting with the anti-ATG5 rabbit polyclonal (Cell Signalling # 2630) and anti-ATG7 rabbit polyclonal (Cell Signalling # 2631) antibodies.

For stable ATG7 downregulation, SO and ATG7 shRNA pGIPZ vectors were purchased from Open Biosystems. Lentivirus supernatants were prepared following the manufacturer's instructions and lentiviral infections carried out accordingly.

Acknowledgments

We thank Dr Craig Thompson for the kind gift of plasmid MigRI–eGFP-LC3 and Dr Elisabeth Buchdunger (Novartis) for the kind gift of IM. We also thank Marja Jaattela (Danish Cancer Society, Copenhagen, Denmark), Gerry Cohen, Ed Bampton, Mario Rossi, Gerry Melino and Melania Capasso (MRC Toxicology Unit, Leicester, UK), Tommaso Zanocco (University of Modena and Reggio Emilia, Modena, Italy) for reagents and critical discussion. P.S., A.H. and G.V.H. were supported by the Medical Research Council, UK. A.H. was partly funded by the Leukaemia Research Fund, UK. T.S. is an MSc student at the University of Modena and Reggio Emilia, Modena, Italy. This work was supported, in part, by NCI grant PO1 CA78890 to B.C. M.R.L. and A.R.S were supported, in part, by a fellowship of the American-Italian Foundation for Cancer Research (AIFCR). C.B. was the recipient of a PhD studentship at the University of Leicester, UK. We thank all the patients and UK haematologists who have provided normal and CML samples for our Biobank.

References

1. Kantarjian, H.M., Keating, M.J., Talpaz, M., Walters, R.S., Smith, T.L., Cork, A., McCredie, K.B., and Freireich, E.J. 1987. Chronic myelogenous leukemia in blast crisis. Analysis of 242 patients. *Am J Med* **83**:445-454.
2. Savage, D.G., Szydlo, R.M., and Goldman, J.M. 1997. Clinical features at diagnosis in 430 patients with chronic myeloid leukaemia seen at a referral centre over a 16-year period. *Br J Haematol* **96**:111-116.
3. Spiers, A.S. 1995. Clinical manifestations of chronic granulocytic leukemia. *Semin Oncol* **22**:380-395.
4. Ben-Neriah, Y., Daley, G.Q., Mes-Masson, A.M., Witte, O.N., and Baltimore, D. 1986. The chronic myelogenous leukemia-specific P210 protein is the product of the bcr/abl hybrid gene. *Science* **233**:212-214.
5. Cortez, D., Kadlec, L., and Pendergast, A.M. 1995. Structural and signaling requirements for BCR-ABL-mediated transformation and inhibition of apoptosis. *Mol Cell Biol* **15**:5531-5541.
6. Gordon, M.Y. 1999. Biological consequences of the BCR/ABL fusion gene in humans and mice. *J Clin Pathol* **52**:719-722.
7. Goga, A., McLaughlin, J., Afar, D.E., Saffran, D.C., and Witte, O.N. 1995. Alternative signals to RAS for hematopoietic transformation by the BCR-ABL oncogene. *Cell* **82**:981-988.
8. Skorski, T., Kanakaraj, P., Nieborowska-Skorska, M., Ratajczak, M.Z., Wen, S.C., Zon, G., Gewirtz, A.M., Perussia, B., and Calabretta, B. 1995. Phosphatidylinositol-3 kinase activity is regulated by BCR/ABL and is required for the growth of Philadelphia chromosome-positive cells. *Blood* **86**:726-736.
9. Vivanco, I., and Sawyers, C.L. 2002. The phosphatidylinositol 3-Kinase AKT pathway in human cancer. *Nat Rev Cancer* **2**:489-501.
10. Sebolt-Leopold, J.S., and Herrera, R. 2004. Targeting the mitogen-activated protein kinase cascade to treat cancer. *Nat Rev Cancer* **4**:937-947.
11. Van Etten, R.A. 2007. Oncogenic signaling: new insights and controversies from chronic myeloid leukemia. *J Exp Med* **204**:461-465.
12. Ottmann, O.G., Druker, B.J., Sawyers, C.L., Goldman, J.M., Reiffers, J., Silver, R.T., Tura, S., Fischer, T., Deininger, M.W., Schiffer, C.A., et al. 2002. A phase 2 study of imatinib in patients with relapsed or refractory Philadelphia chromosome-positive acute lymphoid leukemias. *Blood* **100**:1965-1971.
13. Sawyers, C.L., Hochhaus, A., Feldman, E., Goldman, J.M., Miller, C.B., Ottmann, O.G., Schiffer, C.A., Talpaz, M., Guilhot, F., Deininger, M.W., et al. 2002. Imatinib induces hematologic and cytogenetic responses in patients with chronic myelogenous leukemia in myeloid blast crisis: results of a phase II study. *Blood* **99**:3530-3539.
14. Hofmann, W.K., Jones, L.C., Lemp, N.A., de Vos, S., Gschaidmeier, H., Hoelzer, D., Ottmann, O.G., and Koeffler, H.P. 2002. Ph(+) acute lymphoblastic leukemia resistant to the tyrosine kinase inhibitor STI571 has a unique BCR-ABL gene mutation. *Blood* **99**:1860-1862.
15. Branford, S., Rudzki, Z., Walsh, S., Parkinson, I., Grigg, A., Szer, J., Taylor, K., Herrmann, R., Seymour, J.F., Arthur, C., et al. 2003. Detection of BCR-ABL mutations in patients with CML treated with imatinib is virtually always accompanied by clinical resistance, and mutations in the ATP phosphate-

binding loop (P-loop) are associated with a poor prognosis. *Blood* **102**:276-283.
16. Nardi, V., Azam, M., and Daley, G.Q. 2004. Mechanisms and implications of imatinib resistance mutations in BCR-ABL. *Curr Opin Hematol* **11**:35-43.
17. Deininger, M., Buchdunger, E., and Druker, B.J. 2005. The development of imatinib as a therapeutic agent for chronic myeloid leukemia. *Blood* **105**:2640-2653.
18. Soverini, S., Martinelli, G., Rosti, G., Bassi, S., Amabile, M., Poerio, A., Giannini, B., Trabacchi, E., Castagnetti, F., Testoni, N., et al. 2005. ABL mutations in late chronic phase chronic myeloid leukemia patients with up-front cytogenetic resistance to imatinib are associated with a greater likelihood of progression to blast crisis and shorter survival: a study by the GIMEMA Working Party on Chronic Myeloid Leukemia. *J Clin Oncol* **23**:4100-4109.
19. Graham, S.M., Jorgensen, H.G., Allan, E., Pearson, C., Alcorn, M.J., Richmond, L., and Holyoake, T.L. 2002. Primitive, quiescent, Philadelphia-positive stem cells from patients with chronic myeloid leukemia are insensitive to STI571 in vitro. *Blood* **99**:319-325
20. Shah, N.P., Tran, C., Lee, F.Y., Chen, P., Norris, D., and Sawyers, C.L. 2004. Overriding imatinib resistance with a novel ABL kinase inhibitor. *Science* **305**:399-401.
21. Weisberg, E., Manley, P.W., Breitenstein, W., Bruggen, J., Cowan-Jacob, S.W., Ray, A., Huntly, B., Fabbro, D., Fendrich, G., Hall-Meyers, E., et al. 2005. Characterization of AMN107, a selective inhibitor of native and mutant Bcr-Abl. *Cancer Cell* **7**:129-141.
22. O'Hare, T., Eide, C.A., and Deininger, M.W. 2007. Bcr-Abl kinase domain mutations, drug resistance, and the road to a cure for chronic myeloid leukemia. *Blood* **110**:2242-2249.
23. Jiang, X., Zhao, Y., Smith, C., Gasparetto, M., Turhan, A., Eaves, A., and Eaves, C. 2007. Chronic myeloid leukemia stem cells possess multiple unique features of resistance to BCR-ABL targeted therapies. *Leukemia* **21**:926-935.
24. Copland, M., Hamilton, A., Elrick, L.J., Baird, J.W., Allan, E.K., Jordanides, N., Barow, M., Mountford, J.C., and Holyoake, T.L. 2006. Dasatinib (BMS-354825) targets an earlier progenitor population than imatinib in primary CML but does not eliminate the quiescent fraction. *Blood* **107**:4532-4539.
25. Jorgensen, H.G., Allan, E.K., Jordanides, N.E., Mountford, J.C., and Holyoake, T.L. 2007. Nilotinib exerts equipotent antiproliferative effects to imatinib and does not induce apoptosis in CD34+ CML cells. *Blood* **109**:4016-4019.
26. Konig, H., Holtz, M., Modi, H., Manley, P., Holyoake, T.L., Forman, S.J., and Bhatia, R. 2008. Enhanced BCR-ABL kinase inhibition does not result in increased inhibition of downstream signaling pathways or increased growth suppression in CML progenitors. *Leukemia* **22**:748-755.
27. Konig, H., Holyoake, T.L., and Bhatia, R. 2008. Effective and selective inhibition of chronic myeloid leukemia primitive hematopoietic progenitors by the dual Src/Abl kinase inhibitor SKI-606. *Blood* **111**:2329-2338.
28. Kroemer, G., and Jaattela, M. 2005. Lysosomes and autophagy in cell death control. *Nat Rev Cancer* **5**:886-897.
29. Klionsky, D.J. 2007. Autophagy: from phenomenology to molecular understanding in less than a decade. *Nat Rev Mol Cell Biol* **8**:931-937.

30. Baehrecke, E.H. 2005. Autophagy: dual roles in life and death? *Nat Rev Mol Cell Biol* **6**:505-510.
31. Kondo, Y., Kanzawa, T., Sawaya, R., and Kondo, S. 2005. The role of autophagy in cancer development and response to therapy. *Nat Rev Cancer* **5**:726-734.
32. Maiuri, M.C., Zalckvar, E., Kimchi, A., and Kroemer, G. 2007. Self-eating and self-killing: crosstalk between autophagy and apoptosis. *Nat Rev Mol Cell Biol* **8**:741-752.
33. Lum, J.J., Bauer, D.E., Kong, M., Harris, M.H., Li, C., Lindsten, T., and Thompson, C.B. 2005. Growth factor regulation of autophagy and cell survival in the absence of apoptosis. *Cell* **120**:237-248.
34. Maclean, K.H., Dorsey, F.C., Cleveland, J.L., and Kastan, M.B. 2008. Targeting lysosomal degradation induces p53-dependent cell death and prevents cancer in mouse models of lymphomagenesis. *J Clin Invest* **118**:79-88.
35. Lum, J.J., DeBerardinis, R.J., and Thompson, C.B. 2005. Autophagy in metazoans: cell survival in the land of plenty. *Nat Rev Mol Cell Biol* **6**:439-448.
36. Degenhardt, K., Mathew, R., Beaudoin, B., Bray, K., Anderson, D., Chen, G., Mukherjee, C., Shi, Y., Gelinas, C., Fan, Y., et al. 2006. Autophagy promotes tumor cell survival and restricts necrosis, inflammation, and tumorigenesis. *Cancer Cell* **10**:51-64.
37. Amaravadi, R.K., Yu, D., Lum, J.J., Bui, T., Christophorou, M.A., Evan, G.I., Thomas-Tikhonenko, A., and Thompson, C.B. 2007. Autophagy inhibition enhances therapy-induced apoptosis in a Myc-induced model of lymphoma. *J Clin Invest* **117**:326-336.
38. Paglin, S., Hollister, T., Delohery, T., Hackett, N., McMahill, M., Sphicas, E., Domingo, D., and Yahalom, J. 2001. A novel response of cancer cells to radiation involves autophagy and formation of acidic vesicles. *Cancer Res* **61**:439-444.
39. Ito, H., Daido, S., Kanzawa, T., Kondo, S., and Kondo, Y. 2005. Radiation-induced autophagy is associated with LC3 and its inhibition sensitizes malignant glioma cells. *Int J Oncol* **26**:1401-1410.
40. Abedin, M.J., Wang, D., McDonnell, M.A., Lehmann, U., and Kelekar, A. 2007. Autophagy delays apoptotic death in breast cancer cells following DNA damage. *Cell Death Differ* **14**:500-510.
41. Kanzawa, T., Germano, I.M., Komata, T., Ito, H., Kondo, Y., and Kondo, S. 2004. Role of autophagy in temozolomide-induced cytotoxicity for malignant glioma cells. *Cell Death Differ* **11**:448-457.
42. Kanzawa, T., Kondo, Y., Ito, H., Kondo, S., and Germano, I. 2003. Induction of autophagic cell death in malignant glioma cells by arsenic trioxide. *Cancer Res* **63**:2103-2108.
43. Berger, Z., Ravikumar, B., Menzies, F.M., Oroz, L.G., Underwood, B.R., Pangalos, M.N., Schmitt, I., Wullner, U., Evert, B.O., O'Kane, C.J., et al. 2006. Rapamycin alleviates toxicity of different aggregate-prone proteins. *Hum Mol Genet* **15**:433-442.
44. Colell, A., Ricci, J.E., Tait, S., Milasta, S., Maurer, U., Bouchier-Hayes, L., Fitzgerald, P., Guio-Carrion, A., Waterhouse, N.J., Li, C.W., et al. 2007. GAPDH and autophagy preserve survival after apoptotic cytochrome c release in the absence of caspase activation. *Cell* **129**:983-997.

45. Calabretta, B., and Perrotti, D. 2004. The biology of CML blast crisis. *Blood* **103**:4010-4022.
46. Sharma, S.V., Gajowniczek, P., Way, I.P., Lee, D.Y., Jiang, J., Yuza, Y., Classon, M., Haber, D.A., and Settleman, J. 2006. A common signaling cascade may underlie "addiction" to the Src, BCR-ABL, and EGF receptor oncogenes. *Cancer Cell* **10**:425-435.
47. Kabeya, Y., Mizushima, N., Yamamoto, A., Oshitani-Okamoto, S., Ohsumi, Y., and Yoshimori, T. 2004. LC3, GABARAP and GATE16 localize to autophagosomal membrane depending on form-II formation. *J Cell Sci* **117**:2805-2812.
48. Kuma, A., Matsui, M., and Mizushima, N. 2007. LC3, an autophagosome marker, can be incorporated into protein aggregates independent of autophagy: caution in the interpretation of LC3 localization. *Autophagy* **3**:323-328.
49. Fader, C.M., Sanchez, D., Furlan, M., and Colombo, M.I. 2008. Induction of autophagy promotes fusion of multivesicular bodies with autophagic vacuoles in K562 cells. *Traffic* **9**:230-250.
50. Kerkela, R., Grazette, L., Yacobi, R., Iliescu, C., Patten, R., Beahm, C., Walters, B., Shevtsov, S., Pesant, S., Clubb, F.J., et al. 2006. Cardiotoxicity of the cancer therapeutic agent imatinib mesylate. *Nat Med* **12**:908-916.
51. Tirasophon, W., Welihinda, A.A., and Kaufman, R.J. 1998. A stress response pathway from the endoplasmic reticulum to the nucleus requires a novel bifunctional protein kinase/endoribonuclease (Ire1p) in mammalian cells. *Genes Dev* **12**:1812-1824.
52. Hoyer-Hansen, M., Bastholm, L., Szyniarowski, P., Campanella, M., Szabadkai, G., Farkas, T., Bianchi, K., Fehrenbacher, N., Elling, F., Rizzuto, R., et al. 2007. Control of macroautophagy by calcium, calmodulin-dependent kinase kinase-beta, and Bcl-2. *Mol Cell* **25**:193-205.
53. Hoyer-Hansen, M., and Jaattela, M. 2007. Connecting endoplasmic reticulum stress to autophagy by unfolded protein response and calcium. *Cell Death Differ* **14**:1576-1582.
54. Deming, P.B., Schafer,Z.T., Tashker,J.S., Potts,M.B., Deshmukh,M., and Kornbluth,S. 2004. Bcr-Abl-mediated protection from apoptosis downstream of mitochondrial cytochrome c release. *Mol Cell Biol* 24: 10289-10299.
55. Cirinna, M., Trotta, R., Salomoni, P., Kossev, P., Wasik, M., Perrotti, D., and Calabretta, B. 2000. Bcl-2 expression restores the leukemogenic potential of a BCR/ABL mutant defective in transformation. *Blood* **96**:3915-3921.
56. Pattingre, S., and Levine, B. 2006. Bcl-2 inhibition of autophagy: a new route to cancer? *Cancer Res* **66**:2885-2888.
57. Puttini, M., Coluccia, A.M., Boschelli, F., Cleris, L., Marchesi, E., Donella-Deana, A., Ahmed, S., Redaelli, S., Piazza, R., Magistroni, V., et al. 2006. In vitro and in vivo activity of SKI-606, a novel Src-Abl inhibitor, against imatinib-resistant Bcr-Abl+ neoplastic cells. *Cancer Res* **66**:11314-11322.
58. Wang, Y, Cai, D, Brendel, C, Barett, C, Erben, P, Manley., P.W., Hochhaus, A, Neubauer, A and Burchert, A. 2007. Adaptative secretion of granulocyte-macrophage colony stimulating factor (GM-CSF) mediates imatinib and nilotinib resistance in BCR/ABL+ progenitors via JAK-2/STAT-5 pathway activation. *Blood* **109**:2147-2155.
59. Gorre, M.E., Mohammed, M., Ellwood, K., Hsu, N., Paquette, R., Rao, P.N., and Sawyers, C.L. 2001. Clinical resistance to STI-571 cancer therapy caused by BCR-ABL gene mutation or amplification. *Science* **293**:876-880.

60. Maekawa, T., Ashihara, E., and Kimura, S. 2007. The Bcr-Abl tyrosine kinase inhibitor imatinib and promising new agents against Philadelphia chromosome-positive leukemias. *Int J Clin Oncol* **12**:327-340.
61. Donato, N.J., Wu, J.Y., Stapley, J., Gallick, G., Lin, H., Arlinghaus, R., and Talpaz, M. 2003. BCR-ABL independence and LYN kinase overexpression in chronic myelogenous leukemia cells selected for resistance to STI571. *Blood* **101**:690-698.
62. Dai, Y., Rahmani, M., Corey, S.J., Dent, P., and Grant, S. 2004. A Bcr/Abl-independent, Lyn-dependent form of imatinib mesylate (STI-571) resistance is associated with altered expression of Bcl-2. *J Biol Chem* **279**:34227-34239.
63. Ptasznik, A., Nakata, Y., Kalota, A., Emerson, S.G., and Gewirtz, A.M. 2004. Short interfering RNA (siRNA) targeting the Lyn kinase induces apoptosis in primary, and drug-resistant, BCR-ABL1(+) leukemia cells. *Nat Med* **10**:1187-1189.
64. Tokarski, J.S., Newitt, J.A., Chang, C.Y., Cheng, J.D., Wittekind, M., Kiefer, S.E., Kish, K., Lee, F.Y., Borzillerri, R., Lombardo, L.J., et al. 2006. The structure of Dasatinib (BMS-354825) bound to activated ABL kinase domain elucidates its inhibitory activity against imatinib-resistant ABL mutants. *Cancer Res* **66**:5790-5797.
65. Soverini, S., Martinelli, G., Colarossi, S., Gnani, A., Rondoni, M., Castagnetti, F., Paolini, S., Rosti, G., and Baccarani, M. 2007. Second-line treatment with dasatinib in patients resistant to imatinib can select novel inhibitor-specific BCR-ABL mutants in Ph+ ALL. *Lancet Oncol* **8**:273-274.
65. Shah, N.P., Skaggs, B.J., Branford, S., Hughes, T.P., Nicoll, J.M., Paquette, R.L., and Sawyers, C.L. 2007. Sequential ABL kinase inhibitor therapy selects for compound drug-resistant BCR-ABL mutations with altered oncogenic potency. *J Clin Invest* **117**:2562-2569.
67. Piwocka, K., Vejda, S., Cotter, T.G., O'Sullivan, G.C., and McKenna, S.L. 2006. Bcr-Abl reduces endoplasmic reticulum releasable calcium levels by a Bcl-2-independent mechanism and inhibits calcium-dependent apoptotic signaling. *Blood* **107**:4003-4010.
68. Law, J.C., Ritke, M.K., Yalowich, J.C., Leder, G.H., and Ferrell, R.E. 1993. Mutational inactivation of the p53 gene in the human erythroid leukemic K562 cell line. *Leuk Res* **17**:1045-1050.
69. Ahuja, H., Bar-Eli, M., Advani, S.H., Benchimol, S., and Cline, M.J. 1989. Alterations in the p53 gene and the clonal evolution of the blast crisis of chronic myelocytic leukemia. *Proc Natl Acad Sci U S A* **86**:6783-6787.
70. Feinstein, E., Cimino, G., Gale, R.P., Alimena, G., Berthier, R., Kishi, K., Goldman, J., Zaccaria, A., Berrebi, A., and Canaani, E. 1991. p53 in chronic myelogenous leukemia in acute phase. *Proc Natl Acad Sci U S A* **88**:6293-6297.
71. Carew, J.S., Nawrocki, S.T., Kahue, C.N., Zhang, H., Yang, C., Chung, L., Houghton, J.A., Huang, P., Giles, F.J., and Cleveland, J.L. 2007. Targeting autophagy augments the anticancer activity of the histone deacetylase inhibitor SAHA to overcome Bcr-Abl-mediated drug resistance. *Blood* **110**:313-322.
72. Cain, K., Brown, D.G., Langlais, C., and Cohen, G.M. 1999. Caspase activation involves the formation of the aposome, a large (approximately 700 kDa) caspase-activating complex. *J Biol Chem* **274**:22686-22692.
73. Ferrari-Amorotti, G., Keeshan, K., Zattoni, M., Guerzoni, C., Iotti, G., Cattelani, S., Donato, N.J., and Calabretta, B. 2006. Leukemogenesis induced

by wild-type and STI571-resistant BCR/ABL is potently suppressed by C/EBPalpha. *Blood* **108**:1353-1362.

74. Bellodi, C., Kindle, K., Bernassola, F., Dinsdale, D., Cossarizza, A., Melino, G., Heery, D., and Salomoni, P. 2006. Cytoplasmic function of mutant promyelocytic leukemia (PML) and PML-retinoic acid receptor-alpha. *J Biol Chem* **281**:14465-14473.
75. Inoue, S., MacFarlane, M., Harper, N., Wheat, L.M., Dyer, M.J., and Cohen, G.M. 2004. Histone deacetylase inhibitors potentiate TNF-related apoptosis-inducing ligand (TRAIL)-induced apoptosis in lymphoid malignancies. *Cell Death Differ* **11 Suppl 2**:S193-206.

Figure legends

Figure 1

Effects of IM treatment on morphology and autophagy in K562 cells

(**A**) Light microscopy images of May-Grunwald-stained untreated or IM-treated K562. Cells were cultured for 36 hours in the absence or presence of 2μM IM and processed for May-Grumwald staining. (**B** and **C**) Reduced size of IM-treated K562 cells. Size of K562 cells treated with zVAD, IM or IM and zVAD was analyzed using a cytofluorimeter. Representative dot plots of physical parameters FSC-H/SSC-H are shown. Yellow arrow indicates a subpopulation of smaller and denser cells in IM/zVAD- treated cultures, while the black arrow shows dying cells after treatment with IM only. In (**C**), representative histograms of the FSC-H parameter are shown. (**D**) Accumulation of autophagosome-associated LC3-II in IM-treated K562 cells. Western blot shows: endogenous LC3-I and LC3-II levels (upper panel) or ectopic eGFP-LC3-I and eGFP-LC3-II expression (lower panel) in extracts from untreated or IM-treated cells (6 hours). Asterisk indicates a non-specific band (lower panel). Actin was measured as loading control. (**E**) Formation of LC3-positive vesicles in IM-treated eGFP-LC3-transduced K562 cells. eGFP-LC3 K562 cells were cultured in the presence or absence of IM and stained with anti-LC3 antibody (red). Nuclei were counterstained with DAPI.

Figure 2

Autophagy in IM-treated 32D-p210$^{BCR/ABL}$ cells.

(**A**) Formation of LC3-positive vacuoles in IM-treated 32D-p210$^{BCR/ABL}$ cells. Cells were treated for 12 hours with 1μM IM and LC3 levels were analyzed by immunofluorescence/confocal microscopy (anti-LC3, red). (**B**) Western blot detection of LC3-I and LC3-II in IM-treated 32D-p210$^{BCR/ABL}$ cells (6 hours). Actin was measured as loading control. (**C**) IL-3 inhibits IM-induced autophagy in eGFP-LC3-transduced 32D-p210$^{BCR/ABL}$ cells. Cells were cultured for 3 and 6 hours in the presence of different concentrations of IL-3 and IM, as indicated. Asterisk denotes a non-specific band. The LC3-I to LC3-II ratio was calculated by densitometric analysis. Actin was measured as loading control. (**D**) LC3-I/II levels in v-Src-transformed 32D cells stably expressing eGFP-LC3. Cells were treated for 6 or 12 hours with the indicated concentrations of IM, and LC3-I/II levels were analyzed by

Western blot using an anti-LC3 antibody. Asterisk indicates a non-specific band. Actin was detected as loading control. (**E**) IM treatment of 32D-T315I $p210^{BCR/ABL}$ cells does not induce autophagy. 32D-T315I $p210^{BCR/ABL}$ cells were treated with 1μM IM and analyzed for LC3-I/II levels. Actin was detected as internal control. (**F**) Expression of T315I c-Abl in 32D-$p210^{BCR/ABL}$ cells does not block IM-induced LC3-II accumulation. $p210^{BCR/ABL}$/T315I c-Abl co-expressing 32D cells were treated with IM and analyzed for LC3-I/II levels. Actin was detected as loading control.

Figure 3

IM-induced autophagy is preceded by ER stress and relies on intracellular calcium. (**A**) Induction of CHOP expression in IM-treated 32D-$p210^{BCR/ABL}$ cells. CHOP mRNA levels were measured by quantitative real-time PCR in cells treated for 1, 3 or 6 hours with 1μM IM. (**B**) Induction of Grp78 expression in IM-treated 32D-$p210^{BCR/ABL}$ cells. Cells were harvested and lysed at the indicated times after the addition of IM. Extracts were probed with anti-GRP78 and anti-Actin as loading control. (**C**) ER Ca^{2+} content was estimated by adding 5μM thapsigargin (a SERCA pump inhibitor) to Fura-2 loaded 32D-$p210^{BCR/ABL}$ cells. The experiment was conducted at 37^{o}C in a Ca^{2+} free buffer. (**D**) Histogram shows mean ± S.E.M. of Ca^{2+} rise evoked by 5μM thapsigargin in 6 separate experiments. * denotes $p < 0.05$ on Students' unpaired t-test. (**E**) Western blot shows LC3-I/II levels in eGFP-LC3 32D-$p210^{BCR/ABL}$ cells treated (6 hours) with the indicated concentration of IM, EGTA and Bapta/AM. The LC3-I/LC3-II ratio was determined by densitometric analysis and normalized according to the levels of β-actin in each sample (lower panel). (**F**) Western blot shows LC3-I/II levels in eGFP-LC3-transduced K562 cells after the indicated treatments (6 hours). The LC3-I/II ratio was determined as in (E).

Figure 4

Inhibition of autophagy potentiates IM-induced cell death in 32D-$p210^{BCR/ABL}$ cells. (**A**) 32D-$p210^{BCR/ABL}$ cells were cultured for 12 hours in the presence or absence of 1μM IM, alone or in combination with 5μM CQ. Cell death was measured by annexin V staining. Values represent the mean ± S.E.M. of 3 independent experiments. Data were analyzed by unpaired *t*-test. (**B**) 32D-$p210^{BCR/ABL}$ cells were treated with 1μM IM (12 hours), alone or in combination with 20nM Ba. Cell death was measured as

above. Values represent the mean ± S.E.M. of 2 independent experiments. (**C**) CQ has no effects in 32D-T315Ip210$^{BCR/ABL}$ cells. 32D-T315Ip210$^{BCR/ABL}$ cells were treated with IM with or without CQ and analyzed for cell death induction as in (A). (**D**) CQ-induced cell death is caspase-independent. 32D-p210$^{BCR/ABL}$ cells were cultured for 6 hours in the presence or absence of different combination of 1μM IM, 50μM ZVADFMK and 5μM CQ. % of cell death was determined as above. Caspase activity was measured in extracts using a DVED-fluorescent substrate (lower panel shaded in blue). (**E**) Bcl-2 does not block CQ-mediated sensitization to IM. 32D-p210$^{BCR/ABL}$ cells ectopically expressing Bcl-2 (Bcl-2 32D-p210$^{BCR/ABL}$) were cultured with 1μM IM alone or in combination with 5μM CQ. Cell death was measured as above. (**F**) Bcl-2 does not block IM-induced LC3-II accumulation. Western blot shows LC3-I/II levels in extracts of Bcl-2 32D- p210$^{BCR/ABL}$ cells treated for 6 or 12 hours with the indicated concentrations of IM. β-actin was detected as loading control.

Figure 5

CQ treatment potentiates the effect of IM in mice inoculated with GFP-LC3 32D-p210BCR/ABL cells.

(**A**) GFP-positive cells in the bone marrow of untreated or treated (CQ, IM or the CQ/IM combination) leukemic mice: (**B**) Cytokine-independent colony formation from bone marrow cells of untreated or treated (CQ, IM, or the CQ/IM combination) leukemic mice.

Figure 6

Inhibition of autophagy increases IM-induced cell death in K562 cells.

(**A**) Effects of CQ in IM-treated K562 cells. Cells were cultured for 48 hours in the presence or absence of 5μM CQ and 2μM IM and cell death was measured by annexin V immunostaining. Values represent the means ± S.E.M. of 3 independent experiments. Data were analyzed by unpaired *t*-test. (**B**) Effects of Bafilomycin A1 on IM-treated K562 cells. Cells were treated with IM and Ba (10 or 20nM), and cell death was measured by annexin V staining. Values represent the means ± S.E.M. of 3 independent experiments. Data were analyzed by unpaired *t*-test. (**C**) CQ potentiates the effect of IM in clonogenic assays. K562 cells were plated in methylcellulose in the absence or in the presence of IM (0.25 or 0.5μM) and CQ (10μM). Colonies were

counted 10 days later. Values (expressed as percentage of control) represent the means ± S.E.M. of 3 independent experiments. (**D**) CQ potentiates the effect of IM in clonogenic assays of IM resistant K562 (K562R) cells. K562R cells were plated in methylcellulose in the absence or in the presence of IM (2.0, 5.0 or 10μM) and CQ (15μM). Colonies were counted 10 days later. Values (expressed as percentage of control) represent the means ± S.E.M. of 2 independent experiments. (**E**-**H**) Transient ATG5 or ATG7 down-regulation enhances IM-induced cell death. K562 cells were transfected with control or ATG5 (**E** and **F**) or ATG7 (**G** and H) siRNAs and analysed for ATG5 (**E**, upper panel) and ATG7 (**G**, upper panel) expression 48 hours post-transfection. Levels of Actin were measured as loading control. Asterisk denotes a non specific band. 48 hours post-transfection, cells were treated with IM and analysed for LC3 and Actin expression (**E** and **G**, lower panels). Cell death was measured by annexin V staining 24 and 40 hours after IM treatment (**F** and **H**). Values represent the means ± S.E.M. of 3 independent experiments. (**I** and **K**) Stable downregulation of ATG7 expression enhances IM-induced cell death. K562 cells were transduced with SO or ATG7 shRNA pGIPZ lentiviral vectors and levels of ATG7 and Actin were measured (**I**). Infected cells were treated with increasing doses of IM and analysed for LC3-II and Actin expression (**I**, lower panel). IM-induced cell death was measured by annexin V staining at 24 and 40 hours (**K**). Values represent the means ± S.E.M. of 3 independent experiments

Figure 7

Autophagy is induced in IM-treated primary CML cells and acts as a survival mechanism.

(**A**) Accumulation of LC3-II in IM-treated CD34+ CML cells. Cells were treated with IM (2μM) or left untreated. Extracts were probed with anti-LC3 and anti-GRB2 antibodies. LC3-II/LC3-I ratio was determined by densitometric analysis. (**B**) CQ potentiates the effect of IM in clonogenic assays. CD34+ CML cells were plated in methylcellulose in the presence or in the absence of IM (0.5 or 1 μM) and CQ (10μM). Colonies were counted 10 days later. Values (expressed as percentage of control) are representative of 3 independent experiments. (**C**) siRNA-mediated down-regulation of ATG5 or ATG7 expression enhances IM-induced inhibition of colony formation. CD34+ CML cells were transfected with control or ATG5 or ATG7

siRNAs and 24 hours later left untreated or treated with IM (1μM). 24 hours later cells were plated in methylcellulose in the presence or absence of IM. Colonies were counted 10 days later. Representative of 2 independent experiments. (D) ATG5 and ATG7 levels in siRNA transfected CML cells. Western blots show ATG5 and ATG7 expression in M351T CML-CP lysates 24 hours after transfection with scrambled or Atg5 or Atg7 specific siRNA. GRB2 levels were measured as loading control. Asterisk denotes a non specific band.

Figure 8

TKI treatment in combination with inhibition of autophagy results in near complete eradication of CML stem cells.

(**A**) Induction of LC3-positive autophagosomes in TKI-treated CML stem cells. CD34+CD38- cells were stained with an anti-LC3 antibody and analyzed by confocal microscopy. Nuclei were stained with DAP; CML-CP CD34+ cells (n=6) were sorted into progenitor (CD34+CD38+) (**B**) and stem (CD34+CD38-) (**B**) cell populations. Cells were left untreated or pre-treated for 48 hours with Imatinib (IM, 0.5 and 2μM), Das (Das, 10 and 150nM) or Nilotinib (2μM) (CD34+CD38+ cells only), either alone or in combination with CQ (10μM) or Ba (20nM). Cells were then plated in methylcellulose in the presence or absence of indicated drug concentrations (as per pre-treatment). Colonies were counted at 14 days and compared to those derived from cells at baseline (cells with no prior culture or treatment) taken as 100%. Values represent the means ± S.E.M. For long –term culture experiments, CML-CP CD34+ cells (n=3) were cultured in SFM with (D) and without (E) growth factors and left untreated or pre-treated for 6 days with TKI (IM, 2μM, or Das,150 nM) or CQ (10μM) alone, or the TKI/CQ combination, before being added to the LTC-IC feeders. Resulting colonies were compared to thosederived from cells at baseline (cells with no prior culture or treatment) and taken as 100%. Values represent the means ± S.E.M. Panel 8E is presented on a logarithmic scale due to the great differences between baseline and TKI/combination-treated arms.

Figure 9

Inhibition of autophagy potentiates IM-induced cell death in CML cells.

In addition to programmed cell death, inhibition of BCR/ABL causes autophagy, which acts as a survival mechanism in CML cells. Treatment with autophagy inhibitors such as CQ results in potentiation of IM-induced cell death.

Bellodi et al. Fig. 1

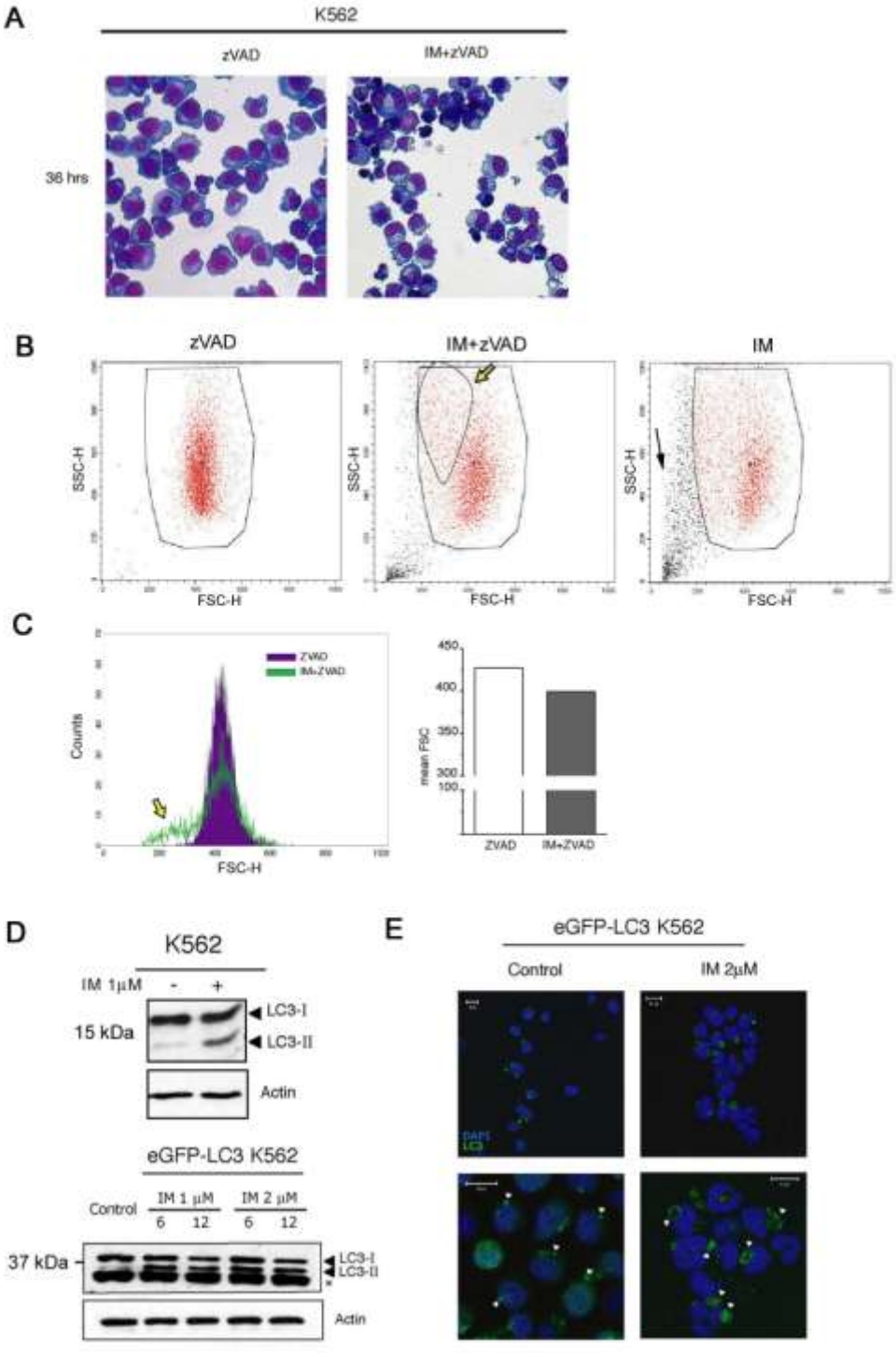

Bellodi et al. Fig. 2

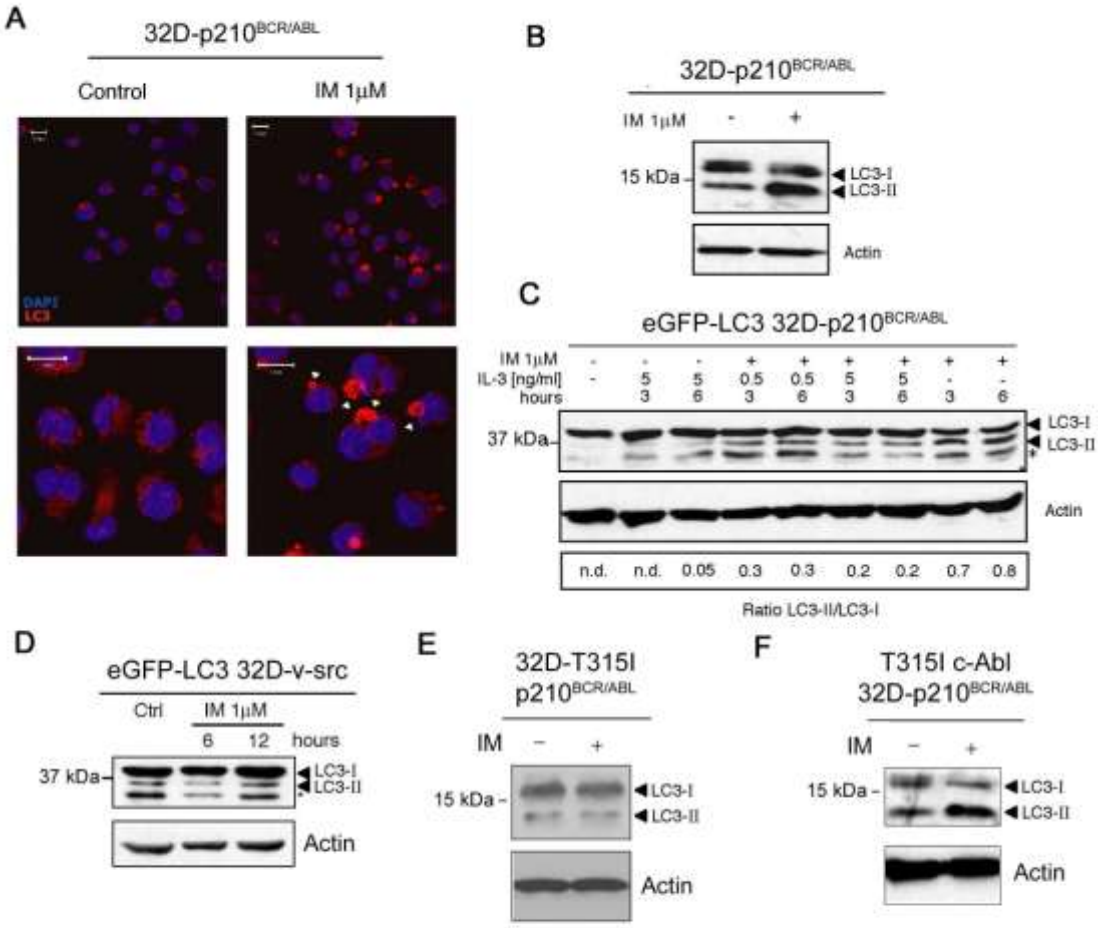

Bellodi et al. Fig. 3

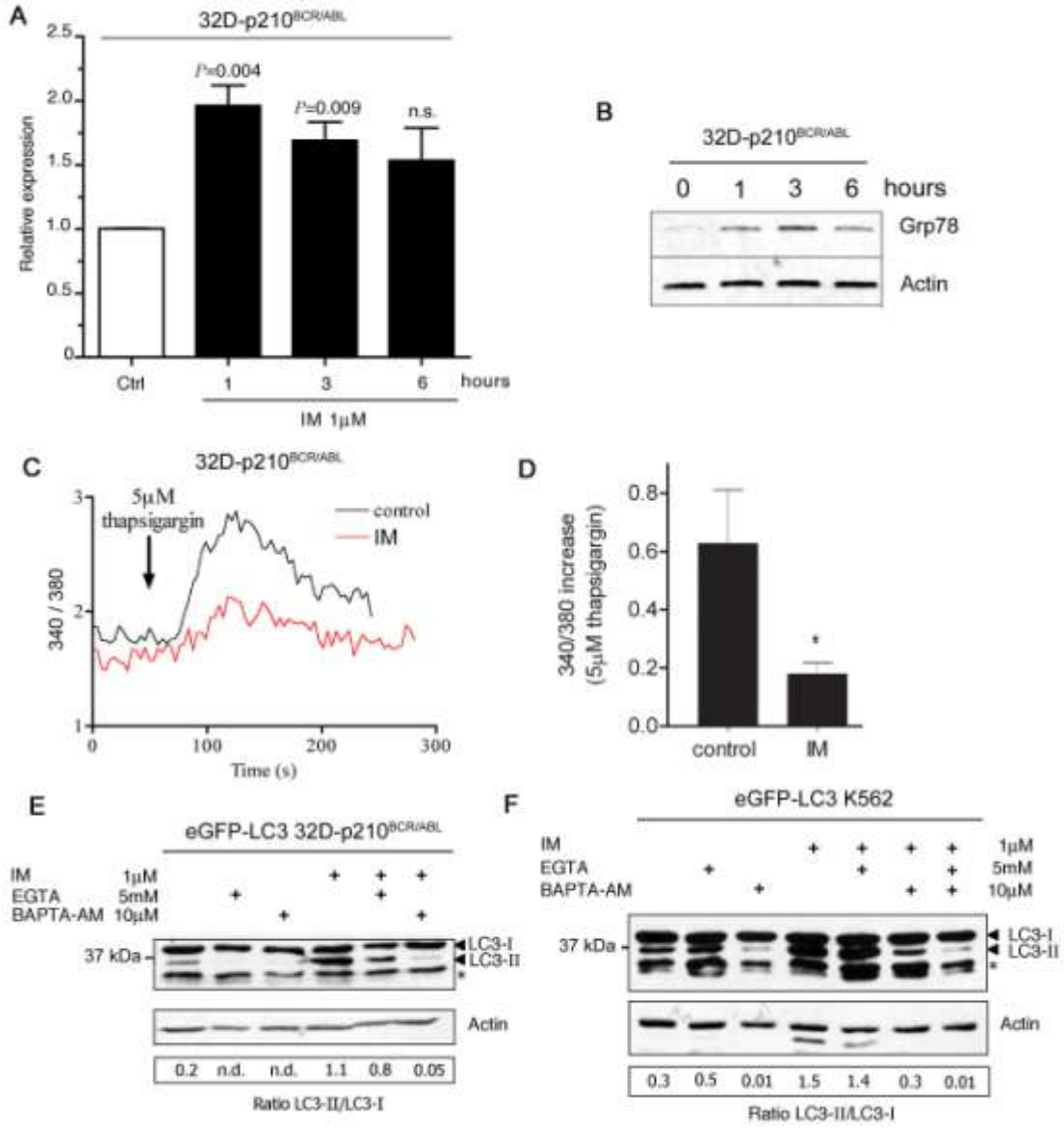

Bellodi et al. Fig. 4

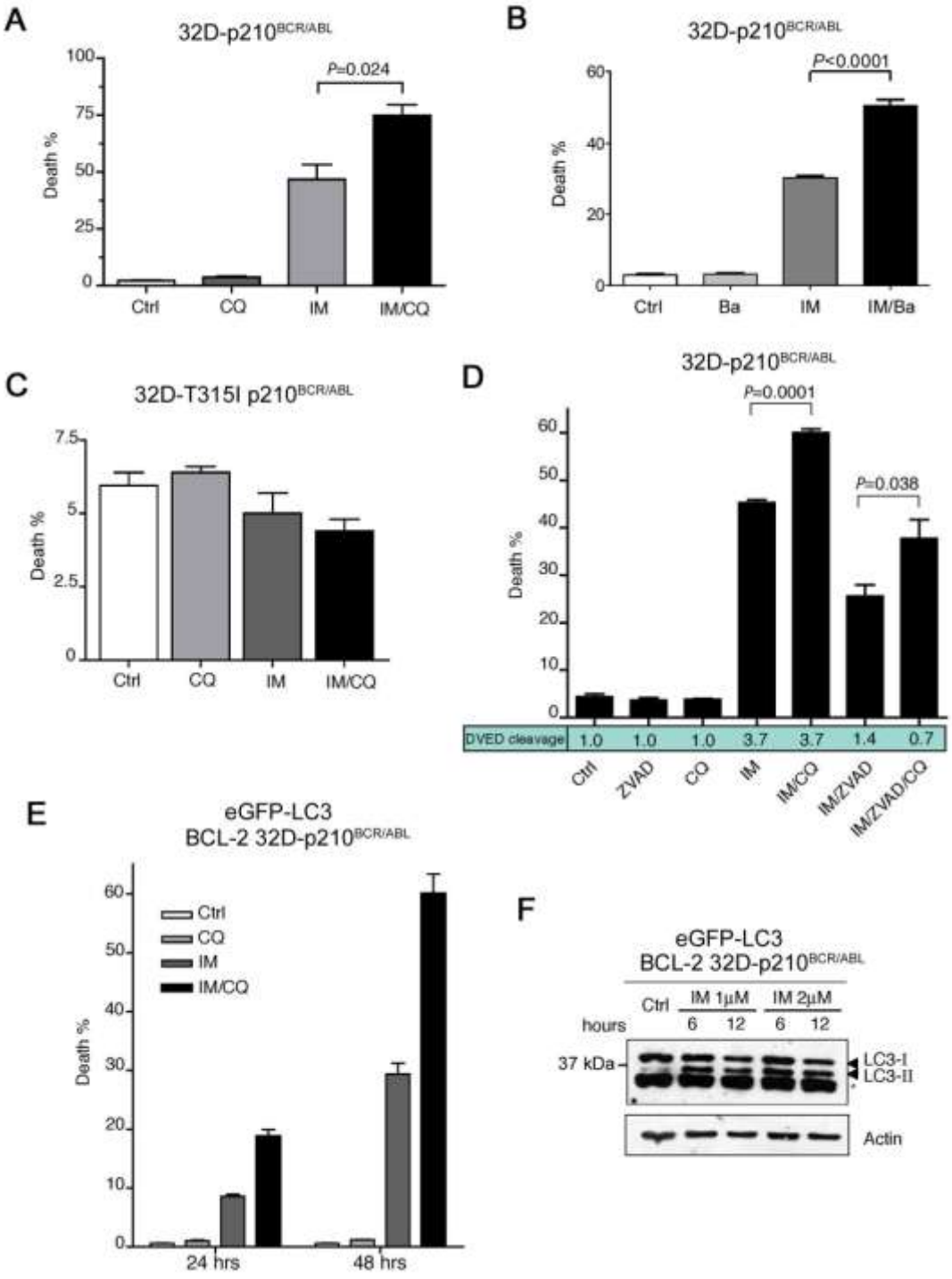

Bellodi et al Fig. 5

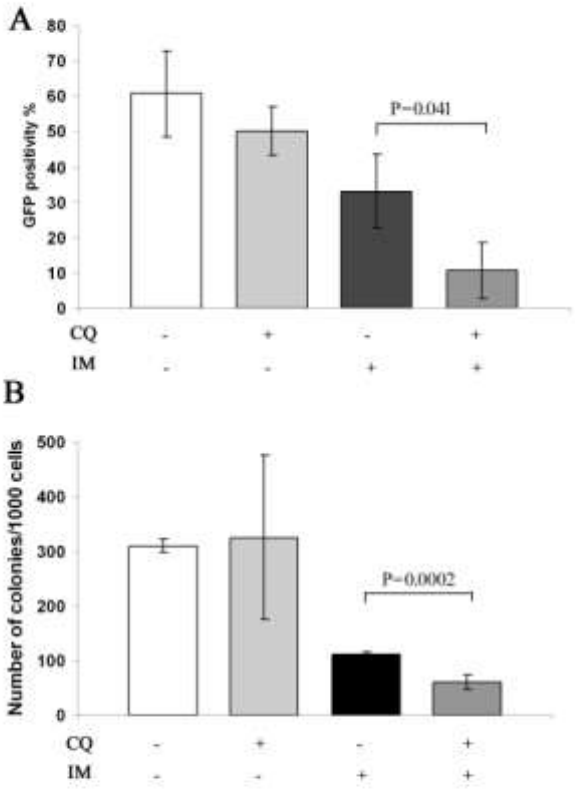

Bellodi et al. Fig. 6

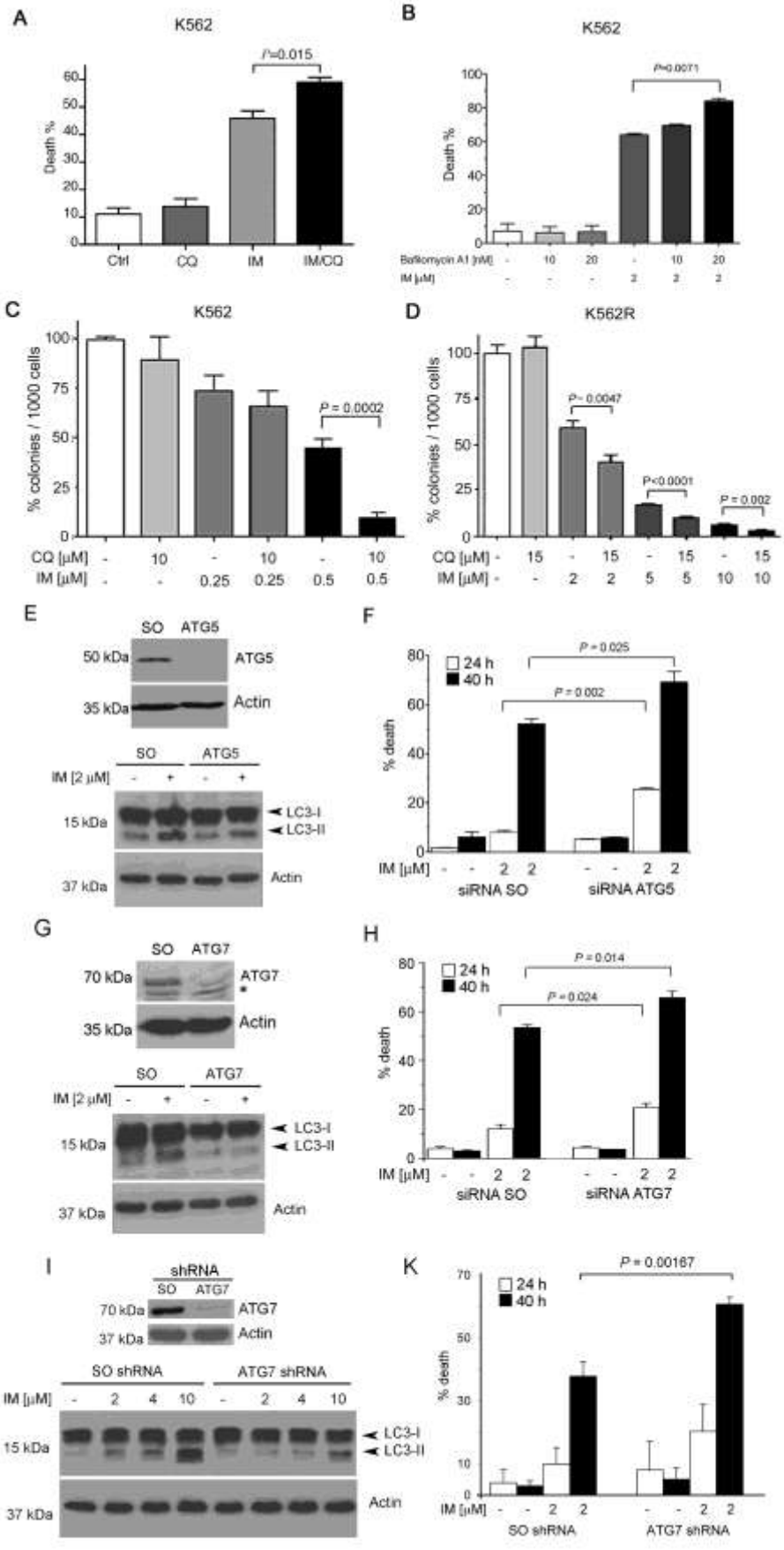

Bellodi et al Fig 7

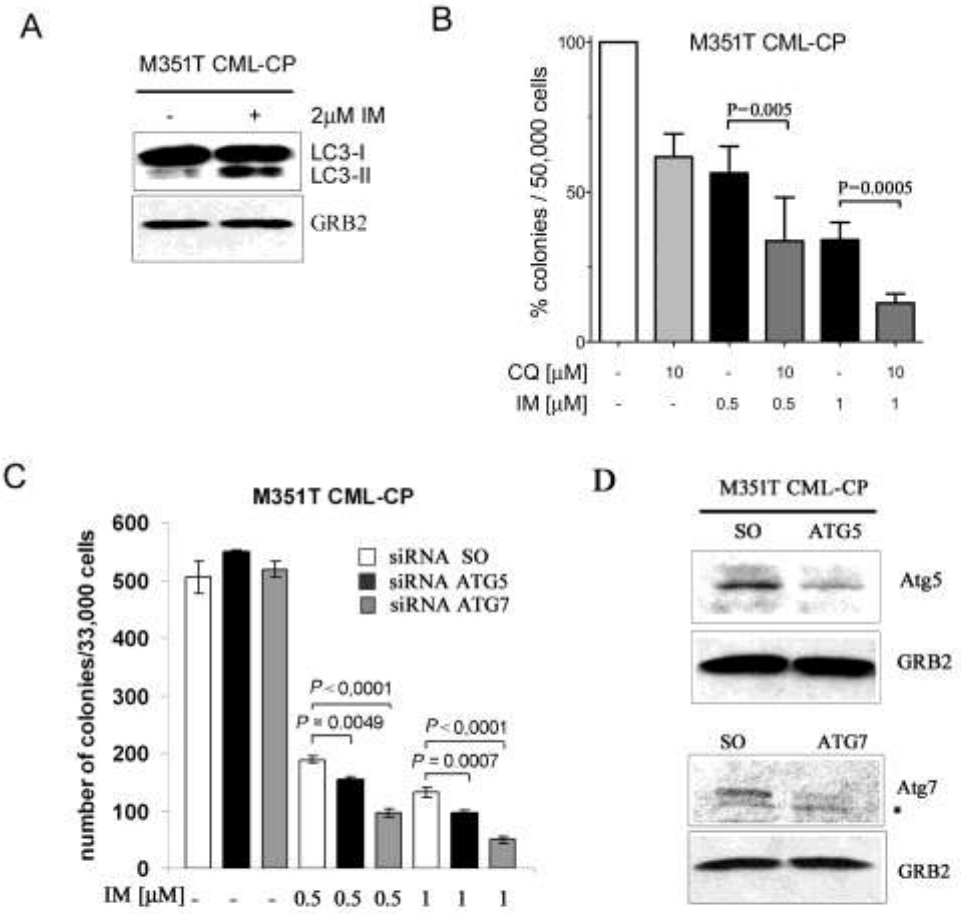

Bellodi et al Fig 8

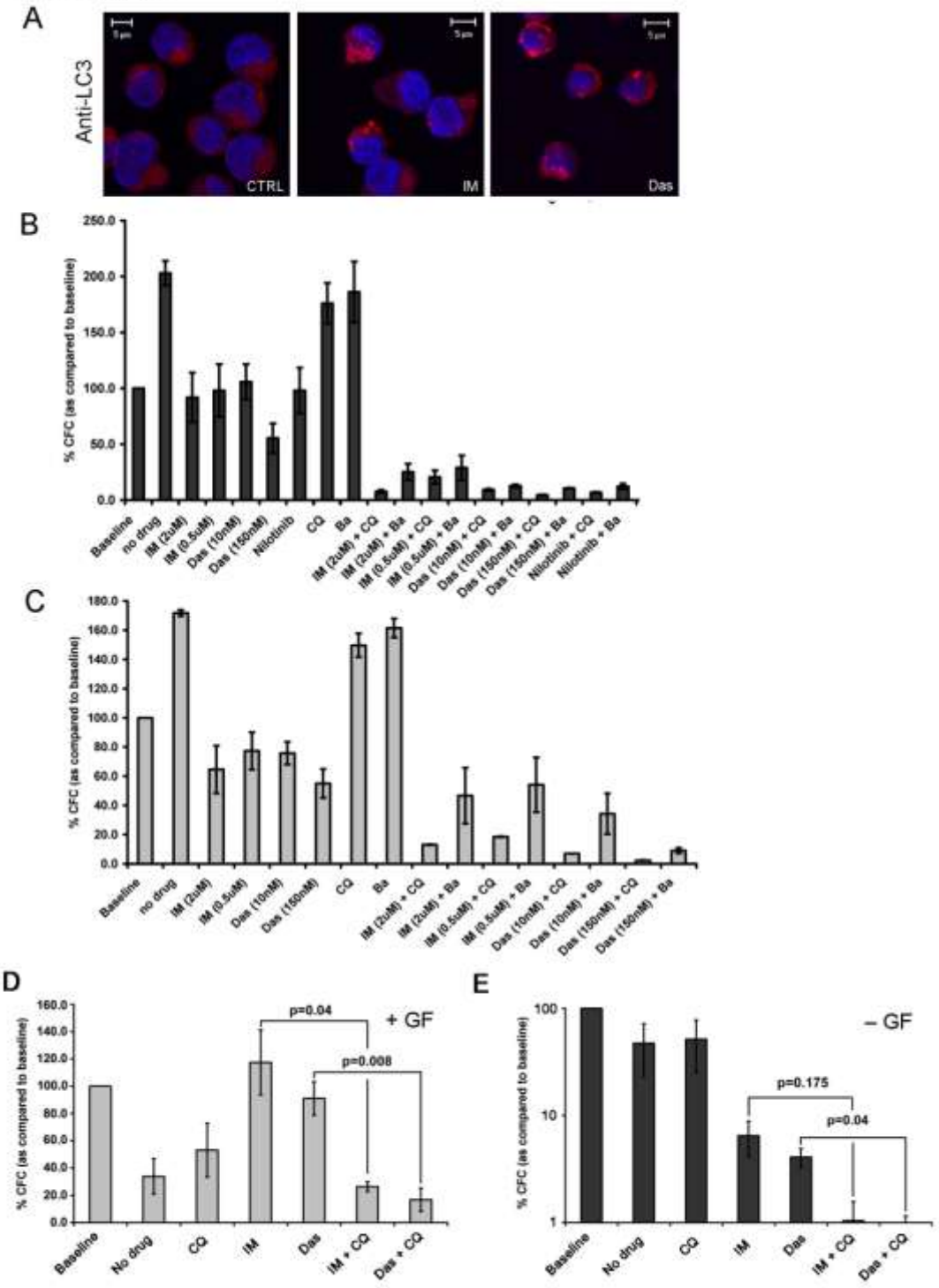

Bellodi et al. Fig. 9